THE EUROPEAN
PHYSICAL JOURNAL C

Regular Article - Experimental Physics

Measurements of W and Z boson production in pp collisions at $\sqrt{s} = 5.02$ TeV with the ATLAS detector

ATLAS Collaboration[*]

CERN, 1211 Geneva 23, Switzerland

Abstract Measurements of fiducial integrated and differential cross sections for inclusive W^+, W^- and Z boson production are reported. They are based on 25.0 ± 0.5 pb^{-1} of pp collision data at $\sqrt{s} = 5.02$ TeV collected with the ATLAS detector at the CERN Large Hadron Collider. Electron and muon decay channels are analysed, and the combined W^+, W^- and Z integrated cross sections are found to be $\sigma_{W^+} = 2266 \pm 9$ (stat) ± 29 (syst) ± 43 (lumi) pb, $\sigma_{W^-} = 1401 \pm 7$ (stat) ± 18 (syst) ± 27 (lumi) pb, and $\sigma_Z = 374.5 \pm 3.4$ (stat) ± 3.6 (syst) ± 7.0 (lumi) pb, in good agreement with next-to-next-to-leading-order QCD cross-section calculations. These measurements serve as references for Pb+Pb interactions at the LHC at $\sqrt{s_{\mathrm{NN}}} = 5.02$ TeV.

1 Introduction

Measurements of $W^\pm$ and Z boson[1] production at hadron colliders provide a benchmark for the understanding of quantum chromodynamics (QCD) and electroweak (EW) processes. Predictions for the differential and fiducial cross sections are available up to next-to-next-to-leading-order (NNLO) accuracy in QCD and include EW corrections at next-to-leading-order (NLO) accuracy [1–3]. The rapidity distribution of EW boson production is sensitive to the underlying QCD dynamics and, in particular, to the parton distribution functions (PDFs) which define the initial kinematics of the hard process. Therefore, measurements of weak-boson production offer an excellent opportunity to test models of parton dynamics.

The ATLAS, CMS and LHCb collaborations have measured $W^\pm$ and Z boson production in proton–proton (pp) collisions at centre-of-mass energies of $\sqrt{s} = 7$, 8 and 13 TeV [4–7]. These measurements provide precision tests of the QCD theory and PDFs, which can be complemented

with measurements at the additional centre-of-mass energy $\sqrt{s} = 5.02$ TeV.

This paper describes measurements of the production cross sections times leptonic branching ratios for the inclusive $W^+ \to \ell^+\nu$, $W^- \to \ell^-\nu$ and $Z \to \ell^+\ell^-$ ($\ell = e$, μ) processes. Integrated and differential cross sections are measured in a fiducial phase space defined by detector acceptance and lepton kinematics. For $W^\pm$ bosons the decay lepton charge asymmetry is also determined. All measurements are performed with pp collision data corresponding to an integrated luminosity of 25.0 pb^{-1}, collected at $\sqrt{s} = 5.02$ TeV with the ATLAS detector. The data were recorded during the autumn of 2015. The peak instantaneous luminosity delivered by the LHC was $L = 3.8 \times 10^{32}$ cm^{-2} s^{-1} and the mean number of pp interactions per bunch crossing (hard scattering and pile-up events) was 1.5. Therefore, this dataset is characterised by a relatively low pile-up contribution as compared to the measurements of weak-boson production performed at higher centre-of-mass energies by ATLAS.

In addition, the measurement of $W^\pm$ and Z boson production in pp collisions at the centre-of-mass energy $\sqrt{s} = 5.02$ TeV is an important reference for weak-boson production in heavy-ion collisions. The LHC has provided both proton–lead (p+Pb) and lead–lead (Pb+Pb) collisions at the centre-of-mass energy per nucleon pair $\sqrt{s_{\mathrm{NN}}} = 5.02$ TeV. Published results from the ATLAS and CMS collaborations are currently available for $W^\pm$ and Z boson production [8–11] in Pb+Pb collisions at $\sqrt{s_{\mathrm{NN}}} = 2.76$ TeV and Z boson production [12,13] in the p+Pb system at $\sqrt{s_{\mathrm{NN}}} = 5.02$ TeV.

2 The ATLAS detector

The ATLAS experiment [14] is a multipurpose particle detector with a forward–backward symmetric cylindrical geometry.[2] It consists of an inner tracking detector surrounded by a

---

[1] Throughout this paper, Z/γ^* boson production is referred to as Z boson production.

[*] e-mail: atlas.publications@cern.ch

---

[2] ATLAS uses a right-handed coordinate system with its origin at the nominal interaction point (IP) in the centre of the detector and the z-axis

Springer

thin superconducting solenoid, electromagnetic and hadronic calorimeters, and a muon spectrometer incorporating three large superconducting air-core toroid magnets with eight coils each.

The inner-detector system (ID) is immersed in a 2 T axial magnetic field and provides charged-particle tracking in the pseudorapidity range $|\eta| < 2.5$. At small radii, a high-granularity silicon pixel detector covers the interaction region and typically provides four measurements per track. It is followed by the silicon microstrip tracker, which usually provides eight measurement points per track. These silicon detectors are complemented by a gas-filled straw-tube transition radiation tracker, which enables track reconstruction up to $|\eta| = 2.0$. The transition radiation tracker also provides electron identification information based on the fraction of hits (out of ~ 35 in total) with an energy deposit above a threshold indicative of transition radiation.

The calorimeter system covers the pseudorapidity range $|\eta| < 4.9$. Within the region $|\eta| < 3.2$, electromagnetic (EM) calorimetry is provided by high-granularity lead/liquid-argon (LAr) calorimeters, with an additional thin LAr presampler covering $|\eta| < 1.8$ to correct for upstream energy-loss fluctuations. The EM calorimeter is divided into a barrel section covering $|\eta| < 1.475$ and two endcap sections covering $1.375 < |\eta| < 3.2$. For $|\eta| < 2.5$ it is divided into three layers in depth, which are finely segmented in η and ϕ. Hadronic calorimetry is provided by a steel/scintillator-tile calorimeter, segmented into three barrel structures within $|\eta| < 1.7$ and two copper/LAr hadronic endcap calorimeters covering $1.5 < |\eta| < 3.2$. The solid-angle coverage is completed with forward copper/LAr and tungsten/LAr calorimeter modules in $3.1 < |\eta| < 4.9$, optimised for electromagnetic and hadronic measurements, respectively.

The muon spectrometer (MS) comprises separate trigger and high-precision tracking chambers measuring the deflection of muons in the magnetic field generated by the toroid magnets. The precision chamber system covers the region $|\eta| < 2.7$ with three layers of monitored drift tubes, complemented by cathode strip chambers in the forward region. The muon trigger system covers the range $|\eta| < 2.4$ with resistive plate chambers in the barrel, and thin gap chambers in the endcap regions.

In 2015, the ATLAS detector had a two-level trigger system [15]. The level-1 trigger is implemented in hardware and uses a subset of detector information to reduce the event rate to a value of at most 75 kHz. This is followed by a software-based high-level trigger which reduces the event rate to about 1 kHz.

3 Simulated event samples

Samples of Monte Carlo (MC) simulated events are used to evaluate the selection efficiency for signal events and the contribution of several background processes to the analysed dataset. All of the samples are processed with the GEANT4-based simulation [16,17] of the ATLAS detector. Dedicated efficiency and calibration studies with data are used to derive correction factors to account for residual differences between experiment and simulation, as is subsequently described.

The processes of interest, specifically events containing $W^{\pm}$ or Z bosons, were generated with the POWHEG-BOX v2 MC program [18] interfaced to the PYTHIA 8.186 parton shower model [19]. The CT10 PDF set [20] was used in the matrix element, while the CTEQ6L1 PDF set [21] was used with the AZNLO [22] set of generator-parameter values (tune) for the modelling of non-perturbative effects in the initial-state parton shower. The PHOTOS++ v3.52 program [23] was used for QED radiation from electroweak vertices and charged leptons. Samples of top-quark pair ($t\bar{t}$) and single-top-quark production were generated with the POWHEG-BOX v2 generator, which uses NLO matrix element calculations together with the CT10f4 PDF set [24]. Top-quark spin correlations were preserved for all top-quark processes. The parton shower, fragmentation, and underlying event were simulated using PYTHIA 6.428 [25] with the CTEQ6L1 PDF set and the corresponding Perugia 2012 tune (P2012) [26]. The top-quark mass was set to 172.5 GeV. The EvtGen v1.2.0 program [27] was used to model bottom and charm hadron decays for all versions of PYTHIA. Diboson processes were simulated using the SHERPA v2.1.1 generator [28]. They were calculated for up to one (ZZ) or zero (WW, WZ) additional partons at NLO QCD accuracy and up to three additional partons at LO. In addition, the SHERPA diboson sample cross section is scaled to account for the cross section change when the G_{μ} scheme [29] is used instead of the native one for the EW parameters, resulting in an effective value of $\alpha \approx 1/132$. Multiple overlaid pp collisions were simulated with the soft QCD processes of PYTHIA v8.186 using the A2 tune [30] and the MSTW2008LO PDF set [31]. For the comparison with data in differential distributions and the evaluation of single-boson EW backgrounds for the cross-section calculations, the single-boson simulations are normalised to the results of NNLO QCD calculations obtained with a modified version of DYNNLO 1.5 [2,3] optimised for speed of computation, with uncertainties of 3%. The simulations of all other processes are normalised to the predictions of NLO QCD calculations, with uncertainties of 10% for the diboson and top-quark processes.

Footnote 2 continued

along the beam pipe. The x-axis points from the IP to the centre of the LHC ring, and the y-axis points upward. Cylindrical coordinates (r, ϕ) are used in the transverse plane, ϕ being the azimuthal angle around the z-axis. The pseudorapidity is defined in terms of the polar angle θ as $\eta = -\ln\tan(\theta/2)$, while the rapidity is defined as $y = \frac{1}{2}\ln\frac{E+p_z}{E-p_z}$.

4 Object definitions and event selection

This section describes the reconstruction of electrons, muons and hadronic recoil objects, and the selection of W and Z bosons. Candidate events are required to have at least one primary vertex reconstructed from at least three tracks with $p_T >$ 400 MeV and to pass a trigger selection, which requires a single electron or muon candidate with a p_T threshold of 15 GeV or 14 GeV, respectively. In addition, a loose likelihood-based identification requirement [32,33] is applied in the electron trigger.

Electron candidates are required to have $p_T >$ 20 (25) GeV in the Z (W) boson analysis and $|\eta| <$ 2.47. Candidates within the transition region between barrel and endcap calorimeters (1.37 $< |\eta| <$ 1.52) are rejected. In addition, medium likelihood-based identification and tight isolation requirements are applied [32,33]. Muon candidates must satisfy $p_T >$ 20 (25) GeV in the Z (W) boson analysis and $|\eta| <$ 2.4 and pass the requirements of medium identification and tight isolation [34]; both criteria were optimised for 2015 analysis conditions.

Additional requirements are imposed on the significance of the transverse impact parameter, d_0, such that $|d_0|/\sigma_{d_0} <$ 5 (3) for electron (muon) candidates. To ensure that lepton candidates originate from the primary vertex, a requirement is also placed on the longitudinal impact parameter, z_0, multiplied by the sine of the track polar angle, θ, such that the absolute value is smaller than 0.5 mm.

Events with Z boson candidates are selected by requiring exactly two opposite-charge electrons or muons, at least one of which is matched to a lepton selected at trigger level. The dilepton invariant mass must satisfy the fiducial requirement 66 $< m_{\ell\ell} <$ 116 GeV.

Events with W boson candidates are selected by requiring exactly one electron or muon that is matched to a lepton selected at trigger level. The (anti-)neutrinos from $W^\pm \rightarrow \ell^\pm \nu$ decays escape direct detection. A measure of the neutrino transverse momentum, p_T^ν, can be inferred from information about the hadronic system recoiling against the W boson. The hadronic recoil is the vector sum of all calorimeter energy clusters excluding the deposits from the decay muon or electron, and is further described below. The transverse projection of the recoil onto the r–ϕ plane, $\vec{u}_T$, is used together with the decay lepton transverse momentum $\vec{p}_T^\ell$ for the calculation of the missing transverse momentum vector,

$$\vec{E}_T^{miss} = - \left(\vec{u}_T + \vec{p}_T^\ell \right),$$

whose magnitude is denoted E_T^{miss}. The transverse mass of the lepton-E_T^{miss} system is defined as $m_T = \sqrt{2 p_T^\ell E_T^{miss} \left(1 - \cos \Delta\phi_{\ell, E_T^{miss}} \right)}$ where $\Delta\phi_{\ell, E_T^{miss}}$ is the azimuthal angle between $\vec{p}_T^\ell$ and $\vec{E}_T^{miss}$. The W boson candidate events are selected by requiring $E_T^{miss} >$ 25 GeV and $m_T >$ 40 GeV. These event selection requirements are optimised to reduce background contributions from multi-jet processes.

The general structure of the algorithm used for hadronic recoil reconstruction is introduced in Ref. [35], where three-dimensional topological clusters [36] calibrated at the hadronic scale are used as inputs to the algorithm. In this measurement, the hadronic recoil is reconstructed using particle flow objects [37] as inputs. The ATLAS particle flow algorithm provides an improved E_T^{miss} resolution compared to the algorithm using only topological clusters, and makes the measurement less sensitive to pile-up by separating the charged-hadron contribution from the neutral hadronic activity [37]. The charged activity is measured by the ID and the related tracks from charged hadrons can be matched to a vertex. From all charged hadrons, only calorimetric clusters associated with a track originating from the reconstructed primary vertex are retained as input to the hadronic recoil algorithm. The neutral hadronic activity is represented by clusters without an associated track, and is also used in the recoil algorithm.

5 Detector performance corrections

5.1 Lepton calibration and efficiency

The electron energy calibration is primarily obtained from the simulation by employing multivariate techniques [38]. The signal $Z \rightarrow ee$ MC simulation is used for deriving the data energy scale calibration and resolution corrections for the simulation. The energy resolution is corrected with additional factors no larger than about 1% in the barrel and up to 2% in the endcap region of the detector in order to account for a slightly worse resolution observed in the data. The energy scale is corrected by applying a per-electron energy scale factor to the data derived from a comparison of the electron-pair invariant mass between the simulation and the data. This procedure was found to be sensitive to the pile-up distribution in data due to different settings used for the signal readout from the EM calorimeters [39]. Therefore, a special set of scale correction factors was derived for this dataset.

Measurements of muon momenta can be biased by the detector alignment and resolution, distortions of the magnetic field or imprecise estimates of the amount of passive material in the detector. Corrections of the muon momentum scale and resolution, which are applied to the simulation, are derived as a function of the muon η and ϕ using $Z \rightarrow \mu^+\mu^-$ events [34]. The correction factors are chosen such that they minimise the χ^2 between the muon-pair invariant mass distributions in data and simulation.

Fig. 1 Efficiencies of reconstruction, identification, isolation and trigger requirements as a function of lepton pseudorapidity for **a** electrons and **b** muons measured using the tag-and-probe method. The efficiency of each selection is defined with respect to leptons selected in the previous step

(a)   **(b)**
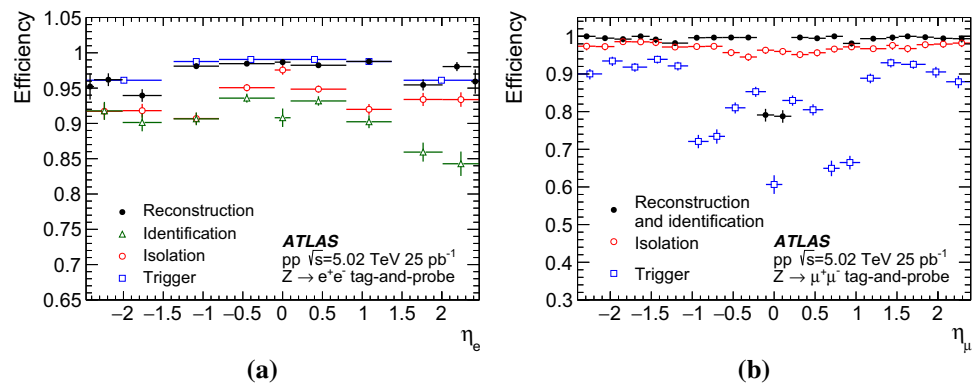
Electron candidates used for the analysis are required to satisfy selection criteria related to reconstruction, identification, isolation and trigger. For each of these requirements, the efficiency of the selection is measured in data with the tag-and-probe method in $Z \rightarrow e^+e^-$ events, as described in Ref. [33], and compared with the simulation. Data-to-simulation ratios of efficiencies are used as scale factors to correct the simulation for the observed differences. Measurements are performed as a function of the electron p_T and η for electrons selected in the analysis. All uncertainties related to efficiency are classified as either correlated or uncorrelated, and are propagated accordingly to the final measurement uncertainty.

The electron reconstruction efficiency is in the range 95–99% both in the data and simulation and is typically measured with a precision of 2%. The data-to-simulation ratio is up to 2% (5%) different from unity in the barrel (endcap) calorimeter and is measured typically with 2% precision for p_T in the range ∼30 to 50 GeV and 5% for $p_T > 60$ GeV. The efficiency of an electron to further pass the medium identification definition varies from 85 to 95% and is measured with 2% precision. This efficiency differs from the efficiency measured in the MC simulation by up to 5%. The isolation efficiency is measured with a precision of 5% and agrees with the simulated value within 2%. Data-to-simulation correction factors for identification and isolation efficiencies are measured with a precision of 2–6%. Finally, the trigger efficiency data-to-simulation ratio is found to deviate from unity by 0.5–3% and is measured with a precision of up to 2%.

Various selection requirements related to muon trigger, reconstruction, identification and isolation are imposed on muon candidates used in the analysis. The efficiency of the selection criteria is measured in data with the tag-and-probe method in $Z \rightarrow \mu^+\mu^-$ events [15,34] and compared with the simulation. Ratios of the efficiencies determined in data and simulation are applied as scale factors to correct the simulated events. For muons with $p_T > 20$ GeV, the correction factors measured as a function of muon p_T have typically an uncertainty of 1–2% and do not deviate from a constant

value by more than 3%. Therefore, the p_T dependence of the scale factors is neglected, and they are evaluated only as a function of muon η.

The muon trigger efficiency in the endcap region of the detector ($1.05 < |\eta| < 2.4$) is measured to be around 90%, and the values obtained in data and simulation agree well. However, in the barrel region ($|\eta| < 1.05$) the trigger efficiency determined in the simulation varies from 70 to 85%, while the efficiency measured in data is lower by 5–15%, which results in sizeable scale factors. The combined reconstruction and identification efficiency for medium-quality muons typically exceeds 99% in both the data and simulation with good agreement between the two measurements. The efficiency of the isolation selection is found to be 97–98% in the MC simulation and it differs from the efficiency measured in the data by about 2% in the most central ($|\eta| < 0.6$) and most forward detector regions ($1.74 < |\eta| < 2.4$).

All measurements of lepton efficiency corrections are limited in their precision by the number of $Z \rightarrow \ell^+\ell^-$ candidates available in the $\sqrt{s} = 5.02$ TeV dataset.

Figure 1 summarises the reconstruction, identification, isolation and trigger efficiencies for electron and muon candidates obtained from the tag-and-probe method.

Figure 2 shows the invariant mass distribution of the dilepton system for electron and muon candidates from $Z \rightarrow \ell^+\ell^-$ boson decays after applying scale factors to the MC simulation. The data points are compared with simulation including Z boson signal and background components. The electron candidates in the data, shown on the left panel, are calibrated using calorimeter settings and calibration correction factors optimised for low-pile-up conditions. Good agreement between the data and the simulation is found for both channels.

5.2 Recoil calibration

In events with W or Z boson production, the hadronic recoil gives a measure of the boson transverse momentum. The calibration of the recoil is performed using dilepton

Fig. 2 Detector-level invariant mass distribution of **a** dielectron and **b** dimuon pairs from Z boson decays together with EW background contributions. Background contributions are too small to be visible on a linear scale. Only the statistical uncertainties of the data are shown
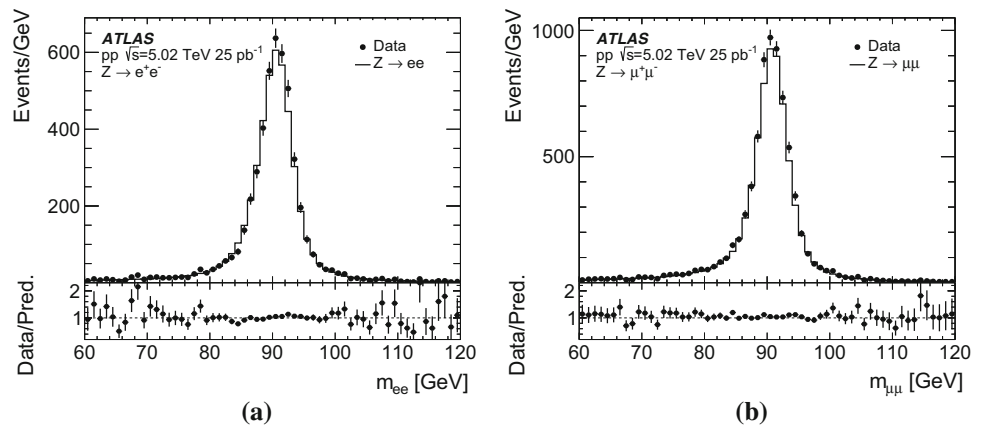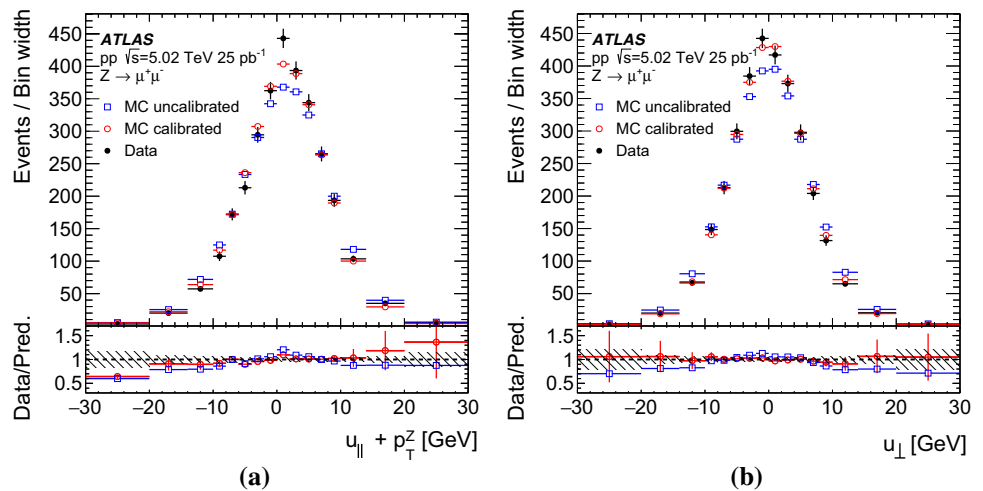

(a)

(b)

Fig. 3 Distributions of **a** $u_\parallel + p_T^Z$ and **b** $u_\perp$ in data and $Z \to \mu^+\mu^-$ MC simulation before (squares) and after (circles) recoil calibration. The shaded band in the ratio panels represents the statistical uncertainty of the data sample, while the error bars represent the systematic uncertainty associated with the calibration procedure

(a)

(b)

events from decays of Z bosons produced in pp collisions at $\sqrt{s} = 5.02$ TeV, as information about the Z boson transverse momentum can be obtained with high precision from the measurements of lepton momenta and compared with the measurement from hadronic recoil. The recoil resolution is studied using $u_\perp$, the projection of $\vec{u}_T$ onto the axis – in the transverse plane – perpendicular to the Z boson $\vec{p}_T$. The resolution is given by the standard deviation of the $u_\perp$ distribution, $\sigma_{u_\perp}$. The transverse momentum scale response of the recoil can be studied using the bias defined as $u_\parallel + p_T^Z$, where $u_\parallel$ is the projection of $\vec{u}_T$ onto the axis defined by $\vec{p}_T^Z$, and is quantified via the average of the bias distribution. Differences between the responses in data and simulation are less than ∼2 GeV, while up to ∼20% differences in the resolution are observed.

Following the procedure described in Ref. [35], in situ corrections to the resolution and the scale of u_T are obtained in Z events and are applied to the W boson event candidates, as a function of p_T^W. The corrections applied to the simulation are obtained as a function of p_T^Z:

$$u_\parallel^{W,\text{corr}} = \left\langle u_\parallel^Z + p_T^Z \right\rangle^{\text{data}} - \left\langle u_\parallel^Z + p_T^Z \right\rangle^{\text{MC}} + \left\langle u_\parallel^{Z,\text{data}} \right\rangle$$
$$+ \left(u_\parallel^{W,\text{MC}} - \left\langle u_\parallel^{Z,\text{data}} \right\rangle \right) \cdot \frac{\sigma_{u_\perp}^{\text{data}}}{\sigma_{u_\perp}^{\text{MC}}}; \tag{1}$$

$$u_\perp^{W,\text{corr}} = u_\perp^{W,\text{MC}} \cdot \frac{\sigma_{u_\perp}^{\text{data}}}{\sigma_{u_\perp}^{\text{MC}}}. \tag{2}$$

Equation (1) describes corrections applied to the recoil response in simulation. It includes a shift which brings the average value of $u_\parallel$ in the simulation closer to the one in data, taking into account differences in the bias. In addition, it corrects the response distribution for resolution differences (last term in the equation). The resolution correction is directly described by Eq. (2) where it is applied to the $u_\perp$ distribution in the simulation. The impact of the calibration on the scale and resolution in events where a Z boson decays to a dimuon pair is shown in Fig. 3. The distributions are shown for the simulation before and after applying the corrections and for data. Agreement of the distributions from simulation with data distributions is improved after applying the calibra-

tion, and residual differences are covered by the systematic uncertainties described in Sect. 8.

6 Background determination

6.1 *W* channels

The reported cross-section measurements correspond to inclusive Drell–Yan production of single vector bosons which decay leptonically. Background processes that contribute to the $W^{\pm}$ boson production measurement are EW processes producing $W^{\pm} \to \tau^{\pm} \nu$, $Z \to \ell^+ \ell^-$, $Z \to \tau^+ \tau^-$ decays, EW diboson (WW, WZ, ZZ) production, as well as top-quark production and multi-jet processes. The multi-jet background includes various processes such as semileptonic decays of heavy-flavour hadrons or in-flight decays of kaons and pions for the muon channel, as well as photon conversions or misidentified hadrons for the electron channel. The background contributions from EW and top-quark production are evaluated using simulated event samples, while the multi-jet contribution is estimated with a data-driven method similar to the one described in Ref. [5].

Although multi-jet background events are well rejected by the lepton isolation requirements, their contribution to the signal region is still sizeable because of the very large production cross sections for multi-jet processes. This contribution is estimated from template fits to data in kinematic distributions: lepton p_T, E_T^{miss} and m_T. The fits are performed in a phase-space region defined by the full event selection with a looser lepton p_T requirement of $p_T > 20$ GeV and with the requirements on E_T^{miss} and m_T removed. An additional requirement on the transverse component of the hadronic recoil, $u_T < 30$ GeV, is placed to ensure better agreement of the event kinematics between the fit region and the signal region.

Template distributions for signal, EW and top-quark background processes are constructed by applying the fit-region selection to samples of simulated events. Templates enriched in contributions from multi-jet processes are built using events in data with non-isolated leptons selected by inverting the isolation requirement described in Sect. 4. The normalisation factors of template distributions for signal, EW and top-quark backgrounds, as well as the multi-jet background, are extracted from a fit to the data. The fits are repeated with multi-jet background templates constructed from different intervals in a track-based (muon channel) or calorimeter-based (electron channel) isolation variable. Finally, a linear extrapolation to the signal region is performed as a function of the selected isolation variable, accounting also for the difference in kinematic selections between the fit region and the signal region. Examples of post-fit template E_T^{miss} distributions, which are used to extract multi-jet yields in the electron and muon channels, are presented in Fig. 4.

Following this procedure, multi-jet background processes are estimated to contribute around 0.9% of the $W^+ \to e^+ \nu$ sample and 1.4% of the $W^- \to e^- \nu$ sample, while in the muon channel they represent around 0.1% of the $W^+ \to \mu^+ \nu$ sample and 0.2% of the $W^- \to \mu^- \nu$ sample.

The largest background contributions to the decay modes studied come from the production of single EW bosons decaying via other decay channels. The $Z \to e^+ e^-$ background represents 0.1% of the $W^+ \to e^+ \nu$ sample and 0.2% of the $W^- \to e^- \nu$ sample, while the $Z \to \mu^+ \mu^-$ background amounts to 2.8% and 3.8% in the $W^+ \to \mu^+ \nu$ and $W^- \to \mu^- \nu$ samples, respectively. The $W^{\pm} \to \tau^{\pm} \nu$ background contributes around 1.8% to the samples selected in both channels and the $Z \to \tau^+ \tau^-$ background contributes approximately 0.1%. Contributions from top-quark production ($t\bar{t}$ and single top quarks) are estimated to be at the level of 0.1–0.2% in both channels. Similarly, diboson processes represent approximately 0.1% of the selected event samples.

Figures 5 and 6 show detector-level lepton pseudorapidity distributions for positive and negative electron and muon candidates from W boson decays. Good agreement is found between the data and the sum of signal and background contributions.

Fig. 4 Distributions of E_T^{miss} used to extract multi-jet yields in the **a** electron and **b** muon channels after performing the template fits. Only the statistical uncertainties of the data are shown
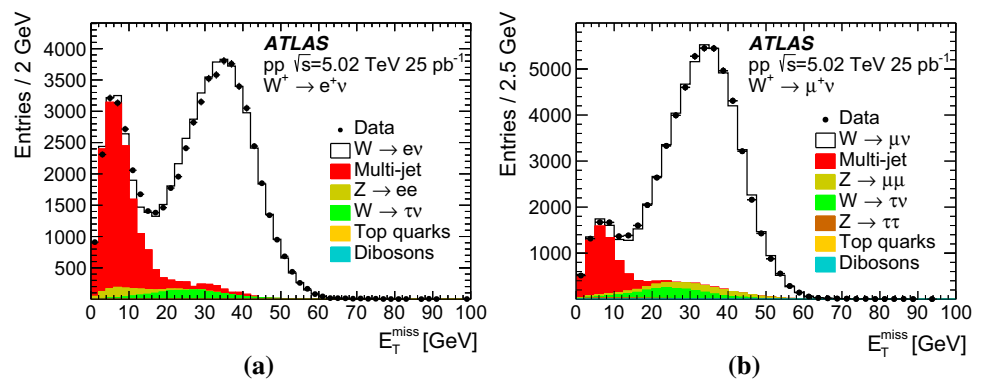
Fig. 5 Distribution of detector-level lepton pseudorapidity for **a** $W^+ \to e^+\nu$ and **b** $W^- \to e^-\nu$. Only the statistical uncertainties of the data are shown
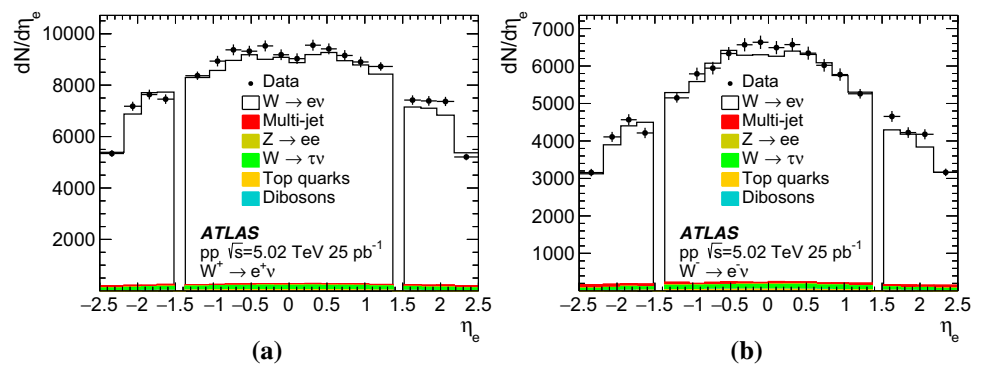
Fig. 6 Distribution of detector-level lepton pseudorapidity for **a** $W^+ \to \mu^+\nu$ and **b** $W^- \to \mu^-\nu$. Only the statistical uncertainties of the data are shown
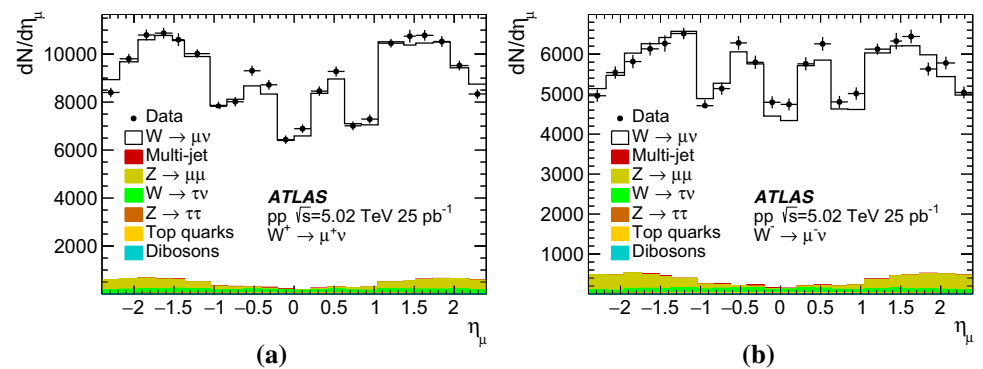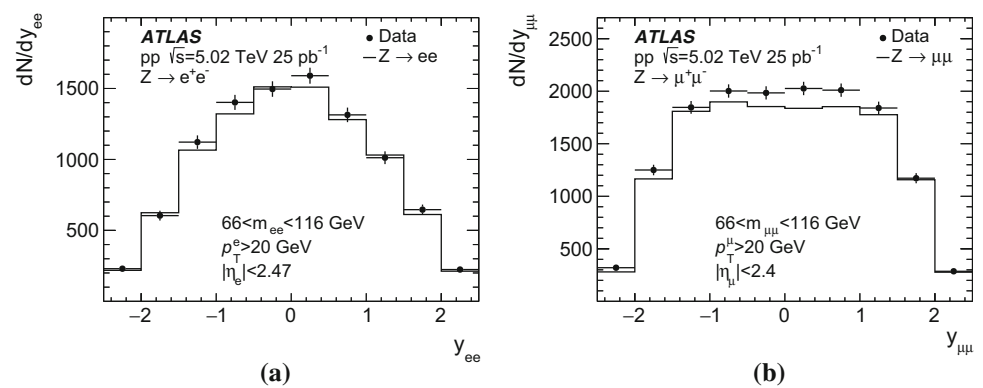
Fig. 7 Detector-level lepton-pair rapidity distributions in the **a** electron and **b** muon channels. Background contributions are negligible using a linear scale. Only the statistical uncertainties of the data are shown

6.2 Z channels

Background contributions to the Z boson sample are expected from $Z \to \tau^+\tau^-$, diboson and W boson decay processes, top-quark pair production, and the multi-jet background. The EW and top-quark contributions are evaluated from dedicated simulation samples, whereas the upper limit on the amount of the multi-jet background is estimated.

Diboson background contributes 0.08% in the muon channel and 0.14% in the electron channel. The $Z \to \tau^+\tau^-$ background is found to be at the level of 0.07% in both decay channels. The top-quark background is at the level of 0.06% in the electron channel and 0.08% in the muon channel. The W boson background is found to be below 0.01% in both channels.

The contribution of the multi-jet background in the muon channel is estimated from samples that simulate $b\bar{b}$ and $c\bar{c}$ production. The study yields an estimate at the level of < 0.01%. A previous ATLAS measurement at $\sqrt{s} = 7$ TeV [4] estimated the multi-jet contribution at the level of 0.02–0.15% for the electron channel and 0.09% for the muon channel. As it is expected that this contribution increases with pile-up and since that measurement was done with higher pile-up than the current analysis, the multi-jet background is considered to be negligible in this analysis.

Figure 7 shows detector-level dilepton rapidity distributions for electron and muon candidates from Z boson decays. Good agreement is found between the data and the sum of signal and background contributions.

Table 1 summarises background contributions to the W^+, W^- and Z boson candidate samples.

Table 1 Background contributions as a percentage of the total for the W^+, W^- and Z candidate samples in the electron (muon) channels

Background	$W^+ \to e^+\nu$ $(W^+ \to \mu^+\nu)$ [%]	$W^- \to e^-\nu$ $(W^- \to \mu^-\nu)$ [%]	$Z \to e^+e^-$ $(Z \to \mu^+\mu^-)$ [%]
$Z \to \ell^+\ell^-, \ell = e, \mu$	0.1 (2.8)	0.2 (3.8)	–
$W^\pm \to \ell^\pm\nu, \ell = e, \mu$	–	–	<0.01 (<0.01)
$W^\pm \to \tau^\pm\nu$	1.8 (1.8)	1.8 (1.8)	<0.01 (<0.01)
$Z \to \tau^+\tau^-$	0.1 (0.1)	0.1 (0.1)	0.07 (0.07)
Multi-jet	0.9 (0.1)	1.4 (0.2)	<0.01 (<0.01)
Top quark	0.1–0.2 (0.1–0.2)	0.1–0.2 (0.1–0.2)	0.06 (0.08)
Diboson	0.1 (0.1)	0.1 (0.1)	0.14 (0.08)

7 Measurement procedure

The integrated and differential W and Z boson production cross sections are measured within a fiducial phase space defined as follows:

- for W production: $p_T^\ell > 25$ GeV, $p_T^\nu > 25$ GeV, $|\eta_\ell| < 2.5$, $m_T > 40$ GeV.
- for Z production: $p_T^\ell > 20$ GeV, $|\eta_\ell| < 2.5$, $66 < m_{\ell\ell} < 116$ GeV.

Integrated fiducial cross sections in the electron and muon channels are calculated using:

$$\sigma^{\text{fid}}_{W^\pm \to \ell^\pm\nu[Z \to \ell^+\ell^-]} = \frac{N_{W[Z]} - B_{W[Z]}}{C_{W[Z]} \cdot L_{\text{int}}}, \quad (3)$$

where $N_{W[Z]}$ and $B_{W[Z]}$ are the number of selected events in data and the expected number of background events, respectively. The integrated luminosity of the sample is $L_{\text{int}} = 25.0 \pm 0.5$ pb^{-1}, determined with the method described in Ref. [40]. A correction for the event detection efficiency is applied with the factor $C_{W[Z]}$, which is obtained from the signal simulation described in Sect. 3 as:

$$C_{W[Z]} = \frac{N^{\text{MC,sel}}_{W[Z]}}{N^{\text{MC,fid}}_{W[Z]}}.$$

Here, $N^{\text{MC,sel}}_{W[Z]}$ is the number of events which pass the signal selection at the detector level, corrected for the observed differences between data and simulation such as in reconstruction, identification, isolation, and trigger efficiencies. The denominator $N^{\text{MC,fid}}_{W[Z]}$ is computed applying the fiducial requirements to the generator-level leptons originating from W and Z boson decays. The measurement is corrected for QED final-state radiation effects by applying these requirements to the lepton momenta before photon radiation. The $C_{W[Z]}$ factors also account for the difference in acceptance between detector-level requirements on lepton $|\eta|$ and the fiducial selection of $|\eta_\ell| < 2.5$.

The procedure described above is extended to the measurement of differential cross sections as a function of the decay lepton pseudorapidity in W boson production, and as a function of the lepton-pair rapidity in Z boson production. The dependence of cross sections on these kinematic variables is particularly sensitive to the choice of PDFs. For the measurement of differential cross sections, the formula given in Eq. (3) is adjusted so that the cross sections are divided by the width of the corresponding interval in absolute pseudorapidity or rapidity. For W production, following Ref. [4], the lepton $|\eta|$ boundaries are defined as:

- 0 – 0.21 – 0.42 – 0.63 – 0.84 – 1.05 – 1.37 – 1.52 – 1.74 – 1.95 – 2.18 – 2.50;

for Z boson production, the lepton-pair $|y_{\ell\ell}|$ boundaries are defined as:

- 0 – 0.5 – 1.0 – 1.5 – 2.0 – 2.5.

For the measurement of these cross sections, the $C_{W[Z]}$ factors are computed separately for each lepton $|\eta|$ or $|y_{\ell\ell}|$ interval by applying the corresponding requirements on the reconstructed lepton kinematics in the numerator, and on the generator-level kinematics in the denominator. Migrations between rapidity intervals are negligible due to the very good angular resolution with which charged-particle tracks associated with leptons are reconstructed, and the good lepton momentum and energy resolutions. The $C_{W[Z]}$ factors for the measurements of integrated and differential cross sections are summarised in Table 2.

The uncertainty associated with the $C_{W[Z]}$ correction is dominated by experimental systematic uncertainties, described in Sect. 8. For the differential C_W factors, the relative size of statistical and systematic uncertainties added in quadrature varies in the range 1.1–2.5% (1.7–3%), while the uncertainties in differential C_Z factors are in the range 1.6–3.5% (0.9–1.2%) in the electron (muon) channel.

Table 2 Correction factors $C_{W[Z]}$ used to calculate integrated and differential W and Z boson production cross sections. The integrated $C_{W[Z]}$ factors are shown with the sum in quadrature of statistical and systematic uncertainties. For the differential $C_{W[Z]}$ factors, the spread of values across lepton $|\eta|$ or $|y_{\ell\ell}|$ intervals is shown, while their uncertainties are described in the text

Channel	C_W ($W^+ \to \ell^+\nu$)	C_W ($W^- \to \ell^-\nu$)	C_Z
Integrated cross-section measurements			
Electron channel	0.657 ± 0.006	0.667 ± 0.005	0.522 ± 0.007
Muon channel	0.723 ± 0.011	0.720 ± 0.010	0.780 ± 0.007
Differential cross-section measurements			
Electron channel	0.55–0.80		0.52–0.62
Muon channel	0.55–0.85		0.60–0.82

Uncertainties in $C_{W[Z]}$ of theoretical origin comprise uncertainties induced by the PDFs, by the description of the W and Z boson transverse momentum distributions, by the implementation of the NLO QCD matrix element and its matching to the parton shower, and by the modelling of the parton shower, hadronisation and underlying event. These uncertainties are discussed in Ref. [4], where they are evaluated to be smaller than 0.2% and thus are negligible at the present level of precision. The size of acceptance corrections included in the integrated correction factors is 7% (3%) for the W boson measurements and 14% (5%) for the Z boson measurements in the electron (muon) channel. In the case of differential W boson measurements, only the C_W factor in the interval $2.18 < |\eta_\ell| < 2.5$ includes an acceptance correction of 9% for $W^\pm \to e^\pm\nu$ processes and 40% for $W^\pm \to \mu^\pm\nu$ processes. On the other hand, all differential C_Z factors include an acceptance correction which varies from 6% to 28% for the $Z \to e^+e^-$ channel and up to 53% for the $Z \to \mu^+\mu^-$ channel.

8 Measurement uncertainties

8.1 Lepton calibration and efficiency corrections

Uncertainties in the determination of lepton trigger, reconstruction, identification and isolation efficiency scale factors affect the measurements through the correction factors $C_{W[Z]}$.

The uncertainties of the electron efficiency measurements are divided into contributions correlated across electron η and p_T intervals and uncorrelated ones, and are propagated to the cross-section measurements accordingly. For the $W^\pm \to e^\pm\nu$ channels the efficiency determination contributes a systematic uncertainty of 0.8% to the fiducial cross-section measurements, while for the $Z \to e^+e^-$ channel this contribution is 1.3%. Systematic effects related to the electron p_T scale and resolution are subdominant, yielding an uncertainty at the level of 0.3% for the $W^\pm \to e^\pm\nu$ channels and less than 0.2% for the $Z \to e^+e^-$ channel. Uncertainties

in the modelling of the electron charge identification are at the level of 0.1%, and neglected for the cross section measurements. Their impact on the asymmetry measurements is however sizeable and included in the final results.

In the muon channels, the statistical components of the scale factor uncertainties are propagated to the measurements via MC pseudo-experiments, while systematic components are propagated as a single variation fully correlated across all muon $|\eta|$ intervals. The single largest contribution to the systematic uncertainty of fiducial cross-section measurements in the $W^\pm \to \mu^\pm\nu$ channels is 1.4% and comes from the determination of the muon trigger efficiency. For measurements in the $Z \to \mu^+\mu^-$ channel the largest systematic uncertainty is contributed by the muon isolation efficiency measurement and amounts to 0.7%. Uncertainties coming from the muon p_T scale and resolution are below 0.2% for both $W^\pm \to \mu^\pm\nu$ channels and the $Z \to \mu^+\mu^-$ channel.

8.2 Hadronic recoil corrections

The uncertainty assigned to the hadronic recoil calibration is conservatively defined from the full size of the corrections, which are derived using events with Z boson production. In these events, the impact of the correction on the $u_\perp$ and $u_\parallel + p_T^Z$ distributions varies between a few percent and $\sim 20\%$ in the range $[-15, +15]$ GeV, which dominates the reported cross-section measurements. After applying this correction to events with W^+ and W^- production, the resulting uncertainties on the cross-section measurements are at the level of 0.5% for both the muon and electron channels.

8.3 Background evaluation

Uncertainties in the evaluation of EW and top-quark backgrounds in the $W^\pm \to e^\pm\nu$ and $W^\pm \to \mu^\pm\nu$ channels are estimated by varying the respective normalisation cross sections. For single-boson production, the size of the cross-section variations is obtained from higher-order QCD calculations, while for diboson and top-quark processes the uncertainty in the cross sections is conservatively taken as

Table 3 Measured fiducial $W^+ \to \ell^+ \nu$ differential and integrated cross sections for electron and muon channels

$|\eta_\ell|^{\mathrm{min}}$	$|\eta_\ell|^{\mathrm{max}}$	$W^+ \to e^+\nu$				$W^+ \to \mu^+\nu$			
		$\mathrm{d}\sigma/\mathrm{d}|\eta_\ell|$ [pb]	$\delta\sigma_{\mathrm{stat}}$ [pb]	$\delta\sigma_{\mathrm{syst}}$ [pb]	$\delta\sigma_{\mathrm{lumi}}$ [pb]	$\mathrm{d}\sigma/\mathrm{d}|\eta_\ell|$ [pb]	$\delta\sigma_{\mathrm{stat}}$ [pb]	$\delta\sigma_{\mathrm{syst}}$ [pb]	$\delta\sigma_{\mathrm{lumi}}$ [pb]
0.00	0.21	448	8	10	8	473	9	15	9
0.21	0.42	463	8	10	9	472	8	11	9
0.42	0.63	453	8	10	9	493	8	11	9
0.63	0.84	460	8	10	9	460	9	12	9
0.84	1.05	466	9	11	9	478	9	13	9
1.05	1.37	469	7	10	9	478	6	10	9
1.37	1.52	–	–	–	–	482	9	12	9
1.52	1.74	460	9	14	9	482	7	10	9
1.74	1.95	454	9	14	8	472	8	10	9
1.95	2.18	453	9	14	8	443	7	10	9
2.18	2.50	370	7	14	7	371	7	9	7
0.00	2.50	2243	13	27	42	2303	12	36	44

10%. The resulting uncertainties in the measurements in both the $W^\pm \to e^\pm\nu$ and $W^\pm \to \mu^\pm\nu$ channels are below 0.2%. Uncertainties related to the multi-jet background evaluation arise from the statistical precision of the multi-jet templates and uncertainty in the normalisations of the subtracted EW and top-quark contamination. These contributions are propagated through linear extrapolations over the isolation variables to the signal region. The related uncertainties in the measurements are evaluated to be 0.7–0.8% in the $W^\pm \to e^\pm\nu$ channels and not more than 0.2% in the $W^\pm \to \mu^\pm\nu$ channels.

In both the $Z \to \mu^+\mu^-$ and $Z \to e^+e^-$ channels, the uncertainty associated with the background subtraction is negligible, since all individual background contributions are below 0.2% of the selected data sample.

8.4 Luminosity calibration

Luminosity measurements in ATLAS are calibrated using dedicated van der Meer scans [40]. The analysis of data from the scan performed in pp collisions at $\sqrt{s} = 5.02$ TeV, which uses the LUCID-2 detector for the baseline luminosity measurements [41], yields a relative systematic uncertainty of 1.9% in the measured luminosity. The largest sources of uncertainty are systematic effects related to the van der Meer scan procedure and the long-term stability of the luminosity calibration

9 Results

9.1 Channel combination

Results of measurements in the electron and muon channels are summarised in Table 3 for W^+ boson production, Table 4

for W^- boson production and Table 5 for Z boson production. In these tables, the statistical uncertainty is defined from the variance of the background-subtracted number of observed events, and the systematic uncertainty includes all uncertainty components described above, except for the luminosity uncertainty, which is given separately. The systematic uncertainties coming from lepton efficiency corrections are measured as a function of lepton η and p_T, and include a significant statistical component due to the number of Z events used to derive the corrections. This statistical component is substantially reduced for the integrated cross sections compared to the differential ones.

The data tables provided in this paper contain compact summaries of the measurement uncertainties. A complete breakdown of systematic uncertainties and their correlated components is provided in HEPData [42].

The electron and muon channel measurements are combined using the Best Linear Unbiased Estimate (BLUE) method [43], accounting for the correlations of the systematic uncertainties across the channels and measurement bins. The $|\eta_\ell|$ and $|y_{\ell\ell}|$ distributions for the electron channel, muon channel and combined results are shown in Figs. 8 and 9 for W and Z bosons, respectively, and the results are listed in Tables 6, 7 and 8. In the interval $1.37 < |\eta_\ell| < 1.52$, only the muon channel measurements for W boson production are used. The combination yields $\chi^2/\mathrm{d.o.f} = 19.3/10$ for the W^+ boson results, $\chi^2/\mathrm{d.o.f} = 15.1/10$ for the W^- boson results, and $\chi^2/\mathrm{d.o.f} = 3.0/5$ for the Z boson results. A simultaneous combination of all measurements, accounting for the correlation of the experimental systematic uncertainties between the W and Z measurement results for a given lepton flavour, gives $\chi^2/\mathrm{d.o.f} = 37.5/25$, corresponding to a probability of 5.2%. In view of this remaining discrepancy and of the general trend of the muon channel cross sections to be higher than the electron channel ones, the systematic

Table 4 Measured fiducial $W^- \to \ell^- \nu$ differential and integrated cross sections for electron and muon channels

$|\eta_\ell|^{\min}$	$|\eta_\ell|^{\max}$	$W^- \to e^- \nu$				$W^- \to \mu^- \nu$			
		$d\sigma/d|\eta_\ell|$ [pb]	$\delta\sigma_{\text{stat}}$ [pb]	$\delta\sigma_{\text{syst}}$ [pb]	$\delta\sigma_{\text{lumi}}$ [pb]	$d\sigma/d|\eta_\ell|$ [pb]	$\delta\sigma_{\text{stat}}$ [pb]	$\delta\sigma_{\text{syst}}$ [pb]	$\delta\sigma_{\text{lumi}}$ [pb]
0.00	0.21	322	7	7	6	341	8	10	6
0.21	0.42	316	7	7	6	314	7	6	6
0.42	0.63	303	7	7	6	327	7	6	6
0.63	0.84	294	7	7	6	303	7	7	6
0.84	1.05	300	7	7	6	306	7	8	6
1.05	1.37	280	5	6	5	290	5	5	6
1.37	1.52	–	–	–	–	276	7	6	5
1.52	1.74	270	7	9	5	272	6	5	5
1.74	1.95	260	7	9	5	245	6	5	5
1.95	2.18	255	7	9	5	253	5	5	5
2.18	2.50	220	6	10	4	219	5	5	4
0.00	2.50	1393	10	17	26	1412	9	22	28

Table 5 Measured fiducial $Z \to \ell^+ \ell^-$ differential and integrated cross sections for electron and muon channels

$|y_{\ell\ell}|^{\min}$	$|y_{\ell\ell}|^{\max}$	$Z \to e^+ e^-$				$Z \to \mu^+ \mu^-$			
		$d\sigma/d|y_{\ell\ell}|$ [pb]	$\delta\sigma_{\text{stat}}$ [pb]	$\delta\sigma_{\text{syst}}$ [pb]	$\delta\sigma_{\text{lumi}}$ [pb]	$d\sigma/d|y_{\ell\ell}|$ [pb]	$\delta\sigma_{\text{stat}}$ [pb]	$\delta\sigma_{\text{syst}}$ [pb]	$\delta\sigma_{\text{lumi}}$ [pb]
0.0	0.5	99.9	2.5	1.6	1.9	105.2	2.4	1.1	2.0
0.5	1.0	100.3	2.7	1.6	1.9	101.9	2.3	1.0	1.9
1.0	1.5	89.2	2.7	1.4	1.7	89.8	2.1	0.8	1.7
1.5	2.0	59.6	2.4	1.2	1.1	61.0	1.8	0.6	1.1
2.0	2.5	19.6	1.3	0.7	0.4	20.3	1.2	0.2	0.4
0.0	2.5	369.0	5.3	4.7	6.9	377.9	4.4	3.4	7.1

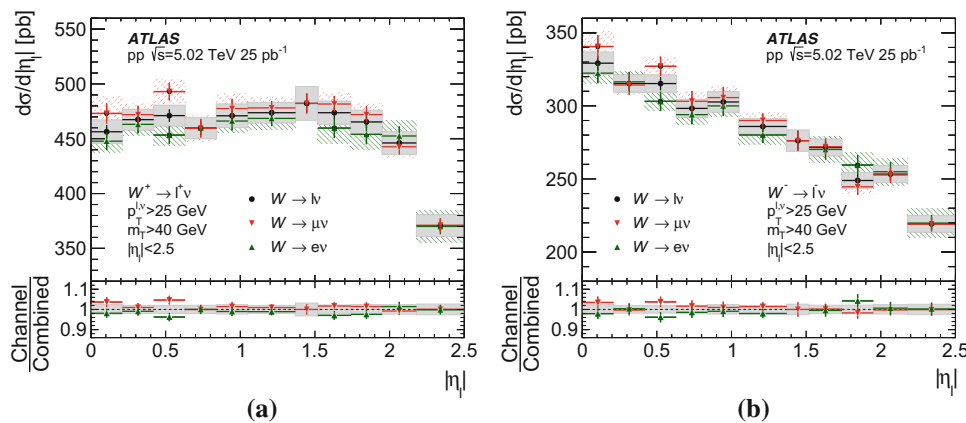**Fig. 8** Differential **a** W^+ and **b** W^- boson production cross sections as a function of absolute decay lepton pseudorapidity, for the electron, muon and combined results. Statistical and systematic errors are shown as corresponding bars and shaded bands. The luminosity uncertainty is not included. The lower panel shows the ratio of channels to the combined differential cross section in each bin. In the lower panel, error bars represent statistical uncertainties in the ratio, while the shaded band represents systematic uncertainties in the combined differential cross sections

uncertainties in the efficiency corrections are scaled such that $\chi^2/\text{d.o.f} = 1$; the correction uncertainties are scaled by a common factor, preserving the uncertainty correlations as a function of lepton p_T and η for this source. Tables 6, 7 and 8 include this scaling. The measured ratio of fiducial W^+ and W^- production cross sections, as well as ratios of fiducial $W^\pm$ and Z production cross sections, are summarised in Table 9.
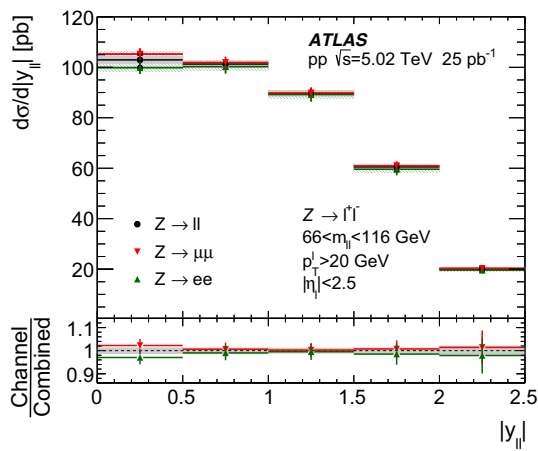
Fig. 9 Differential Z boson production cross section as a function of absolute lepton-pair rapidity, for the electron, muon and combined results. Statistical and systematic errors are shown as corresponding bars and shaded bands. The luminosity uncertainty is not included. The lower panel shows the ratio of channels to the combined differential cross section in each bin. In the lower panel, error bars represent statistical uncertainties in the ratio, while the shaded band represents systematic uncertainties in the combined differential cross sections

Table 6 Combined fiducial $W^+ \rightarrow \ell^+ \nu$ differential and integrated cross sections

$|\eta_\ell|^{\min}$	$|\eta_\ell|^{\max}$	$W^+ \rightarrow \ell^+ \nu$			
		$d\sigma/d|\eta_\ell|$ [pb]	$\delta\sigma_{\mathrm{stat}}$ [pb]	$\delta\sigma_{\mathrm{syst}}$ [pb]	$\delta\sigma_{\mathrm{lumi}}$ [pb]
0.00	0.21	456	6	11	9
0.21	0.42	467	6	9	9
0.42	0.63	471	6	9	9
0.63	0.84	460	6	10	9
0.84	1.05	471	6	11	9
1.05	1.37	474	5	9	9
1.37	1.52	482	9	15	9
1.52	1.74	474	6	11	9
1.74	1.95	465	6	11	9
1.95	2.18	446	6	10	9
2.18	2.50	371	5	10	7
0.00	2.50	2266	9	29	43

Table 7 Combined fiducial $W^- \rightarrow \ell^- \nu$ differential and integrated cross sections

$|\eta_\ell|^{\min}$	$|\eta_\ell|^{\max}$	$W^- \rightarrow \ell^- \nu$			
		$d\sigma/d|\eta_\ell|$ [pb]	$\delta\sigma_{\mathrm{stat}}$ [pb]	$\delta\sigma_{\mathrm{syst}}$ [pb]	$\delta\sigma_{\mathrm{lumi}}$ [pb]
0.00	0.21	329	5	8	6
0.21	0.42	315	5	6	6
0.42	0.63	315	5	6	6
0.63	0.84	298	5	6	6
0.84	1.05	303	5	7	6
1.05	1.37	286	4	5	6
1.37	1.52	276	7	7	5
1.52	1.74	272	4	6	5
1.74	1.95	249	4	5	5
1.95	2.18	253	4	6	5
2.18	2.50	219	4	6	4
0.00	2.50	1401	7	18	27

Table 8 Combined fiducial $Z \rightarrow \ell^+ \ell^-$ differential and integrated cross sections

$|y_{\ell\ell}|^{\min}$	$|y_{\ell\ell}|^{\max}$	$Z \rightarrow \ell^+ \ell^-$			
		$d\sigma/d|y_{\ell\ell}|$ [pb]	$\delta\sigma_{\mathrm{stat}}$ [pb]	$\delta\sigma_{\mathrm{syst}}$ [pb]	$\delta\sigma_{\mathrm{lumi}}$ [pb]
0.0	0.5	103.0	1.7	1.2	1.9
0.5	1.0	101.3	1.8	1.1	1.9
1.0	1.5	89.6	1.7	0.9	1.7
1.5	2.0	60.5	1.4	0.7	1.1
2.0	2.5	20.0	0.9	0.4	0.4
0.0	2.5	374.5	3.4	3.6	7.0

Table 9 Ratios of integrated W and Z production cross sections

$R^{\mathrm{fid}}_{W^+/W^-}$	1.617 ± 0.012 (stat) ± 0.003 (syst)
$R^{\mathrm{fid}}_{W/Z}$	9.81 ± 0.13 (stat) ± 0.01 (syst)
$R^{\mathrm{fid}}_{W^+/Z}$	6.06 ± 0.08 (stat) ± 0.01 (syst)
$R^{\mathrm{fid}}_{W^-/Z}$	3.75 ± 0.05 (stat) ± 0.01 (syst)

The measurements of differential W^+ and W^- production cross sections allow the extraction of the W boson charge asymmetry, as a function of the absolute pseudorapidity of the decay lepton:

$$A_\ell(|\eta_\ell|) = \frac{d\sigma_{W^+}/d|\eta_\ell| - d\sigma_{W^-}/d|\eta_\ell|}{d\sigma_{W^+}/d|\eta_\ell| + d\sigma_{W^-}/d|\eta_\ell|}.$$

Uncertainties in A_ℓ are calculated considering all sources of correlated and uncorrelated systematic uncertainties in the differential cross sections. The resulting dependence of A_ℓ on $|\eta_\ell|$ measured in the electron and muon channels is pre-

sented in Fig. 10 together with the combined values, while the combined results are summarised with the corresponding uncertainties in Table 10. Good agreement between the two channels is found.

9.2 Comparison with theoretical predictions

The measured cross sections are compared with theoretical predictions obtained using a modified version of DYNNLO 1.5 [2,3] optimised for speed of computation. The calculation is performed at $O(\alpha_S^2)$ in QCD and at leading order in the EW theory, with parameters set according to the G_μ scheme [29]. The input parameters (the Fermi constant
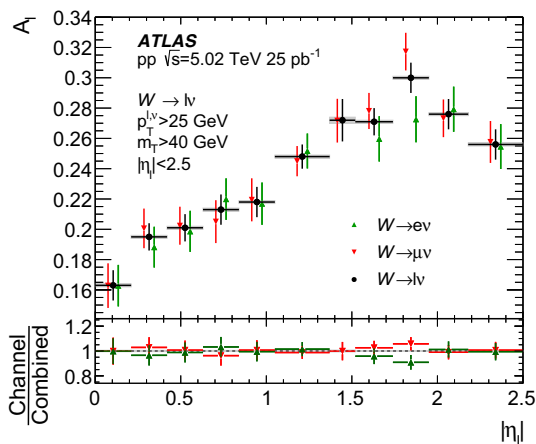
Fig. 10 Charge asymmetry for W bosons as a function of absolute decay lepton pseudorapidity, for the electron, muon and combined results. Statistical and systematic errors are shown as corresponding bars and shaded bands (not visible for most points). The lower panel shows the ratio of channels to the combined charge asymmetry in each bin. In the lower panel, error bars represent statistical uncertainties in the ratio, while the shaded band represents systematic uncertainties in the combined charge asymmetry

Table 10 Charge asymmetry for W bosons as a function of absolute pseudorapidity of the decay lepton

$\|\eta_\ell\|^{\min}$	$\|\eta_\ell\|^{\max}$	A_ℓ	δA_{stat}	δA_{syst}
0.00	0.21	0.163	0.010	0.001
0.21	0.42	0.195	0.009	0.001
0.42	0.63	0.201	0.009	0.001
0.63	0.84	0.213	0.010	0.001
0.84	1.05	0.218	0.010	0.001
1.05	1.37	0.248	0.008	0.001
1.37	1.52	0.272	0.014	0.002
1.52	1.74	0.271	0.009	0.001
1.74	1.95	0.300	0.010	0.001
1.95	2.18	0.276	0.010	0.001
2.18	2.50	0.256	0.010	0.001

G_{F}, the masses and widths of W and Z bosons, and the CKM matrix elements) are taken from Ref. [44]. The DYNNLO predictions are calculated using the NNLO PDF sets from CT14NNLO [45], NNPDF3.1 [46], MMHT14NNLO68CL [47], HERAPDF2.0 [48] and ABMP16 [49]. All considered PDF sets except HERAPDF2.0 are evaluated from global fits which include to varying extents the LHC measurements of W/Z boson, Drell–Yan, top-quark and inclusive jet production. The renormalisation and factorisation scales, respectively denoted as μ_{R} and μ_{F}, are set equal to the decay lepton-pair invariant mass, $m_{\ell\nu}$ or $m_{\ell\ell}$.

Uncertainties in these predictions are derived as follows. PDF uncertainties are evaluated from the variations of the NNLO PDFs (the PDF uncertainties of CT14NNLO

are rescaled from 90% confidence level to 68% confidence level). Scale uncertainties are defined by the envelope of the variations obtained by changing μ_{R} and μ_{F} by a factor of two with respect to their nominal values and imposing $0.5 \leq \mu_{\text{R}}/\mu_{\text{F}} \leq 2$. The uncertainty induced by the strong coupling constant is estimated by varying α_{S} by ± 0.001 around the central value of $\alpha_{\text{S}}(m_Z) = 0.118$, following the prescription of Ref. [45]; the effect of these variations is estimated by comparing the CT14NNLO_AS_0117 and CT14NNLO_AS_0119 PDF sets to CT14NNLO. Finally, intrinsic limitations of the NNLO calculations for fiducial cross-section predictions lead to systematic differences between results from different programs, as explained in Ref. [50]. Therefore, an additional uncertainty of 0.7%, estimated from a comparison of predictions calculated with FEWZ 3.1 and DYNNLO, is assigned. Theory uncertainties are dominated by our knowledge of the proton PDFs.

The uncertainty of the LHC proton beam energy is estimated to be 0.1% [51] and induces typically an uncertainty of 0.1% in the cross-section predictions, which is negligible compared to other theoretical uncertainties discussed above.

Differential cross sections for W and Z boson production are shown in Figs. 11 and 12 as a function of $|\eta_\ell|$ and $|y_{\ell\ell}|$, respectively. The cross sections are compared for the combined measurement and theoretical predictions calculated with the CT14NNLO, NNPDF3.1, MMHT14NNLO68CL, HERAPDF2.0 and ABMP16 PDF sets, with uncertainties assigned as described above. In some regions of phase space, a comparison of the differential cross sections shows systematic deviations of the predictions obtained with recent PDF sets from the measured values. These deviations are largest for W^+ boson production and at central rapidity for Z boson production.

The measured lepton charge asymmetry for W bosons shown in Fig. 13 is compared with predictions calculated with the PDF sets mentioned previously. In most of the $|\eta_\ell|$ range considered, the predictions from all PDF sets tend to underestimate the measured asymmetry by a few percent.

10 Summary

Fiducial cross sections are reported for inclusive W^+, W^- and Z boson production in pp collisions at the centre-of-mass energy $\sqrt{s} = 5.02$ TeV. The measurement is based on data taken by the ATLAS detector at the LHC corresponding to an integrated luminosity of 25.0 pb^{-1}. Cross sections are reported in the electron and muon decay channels, integrated over the fiducial regions and differentially. The fiducial region is defined using lepton kinematics and detector acceptance. The differential cross sections for $W^\pm \to \ell^\pm \nu$ boson production are measured as a function of absolute lepton pseudorapidity while for $Z \to \ell^+\ell^-$ bosons they are

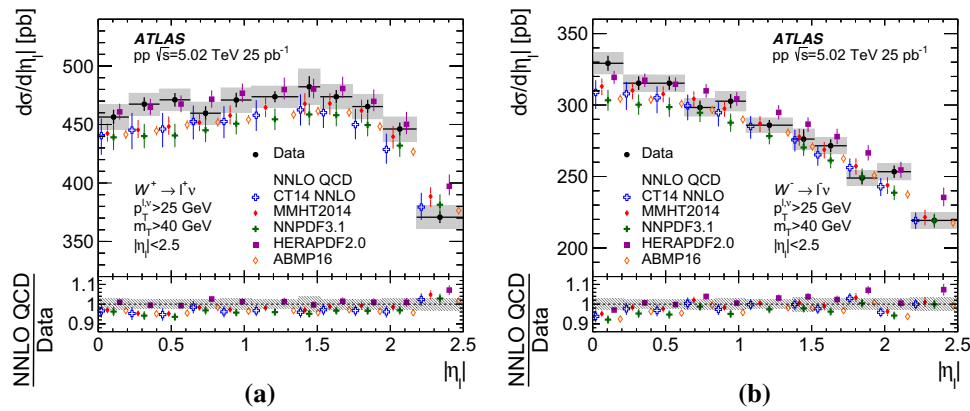**Fig. 11** Differential cross sections for **a** W^+ and **b** W^- boson production as a function of absolute decay lepton pseudorapidity compared with theoretical predictions. Statistical and systematic errors are shown as corresponding bars and shaded bands on the data points. The luminosity uncertainty is not included. Only the dominant uncertainty (PDF) is displayed for the theory. The lower panel shows the ratio of predictions to the measured differential cross section in each bin, and the shaded band shows the sum in quadrature of statistical and systematic uncertainties of the data
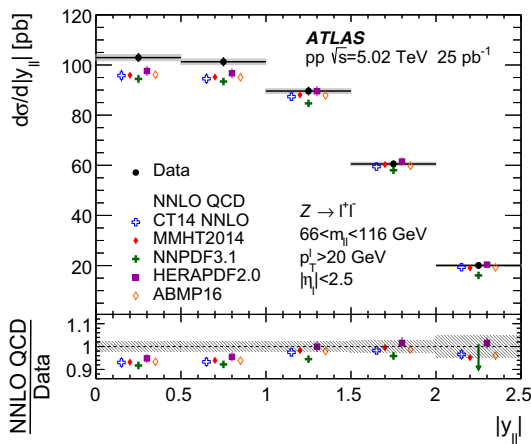

Fig. 12 Differential cross section for Z boson production as a function of absolute lepton-pair rapidity compared with theoretical predictions. Statistical and systematic errors are shown as corresponding bars and shaded bands on the data points. The luminosity uncertainty is not included. Only the dominant uncertainty (PDF) is displayed for the theory. The lower panel shows the ratio of predictions to the measured differential cross section in each bin, and the shaded band shows the sum in quadrature of statistical and systematic uncertainties of the data
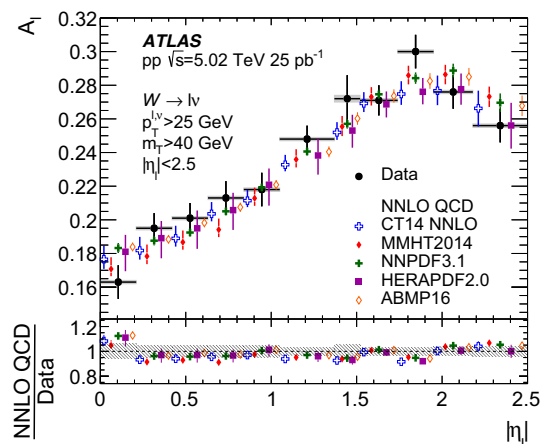

Fig. 13 Charge asymmetry for W bosons as a function of absolute decay lepton pseudorapidity compared with theoretical predictions. Statistical and systematic errors are shown as corresponding bars and shaded bands on the data points. Only the dominant uncertainty (PDF) is displayed for the theory. The lower panel shows the ratio of predictions to the measured differential cross section in each bin, and the shaded band shows the sum in quadrature of statistical and systematic uncertainties of the data

reported as a function of absolute dilepton rapidity in the mass window $66 < m_{\ell\ell} < 116$ GeV. For $W^\pm$ bosons the decay lepton charge asymmetry as a function of absolute lepton pseudorapidity is also measured.

The electron and muon channel results are found to agree within the measurement precision, and are therefore combined considering all sources of correlated and uncorrelated uncertainties. The combined fiducial W^+, W^-, and Z cross sections are measured with a precision of 1.2–1.7%, excluding the luminosity uncertainty. Both the integrated and differential cross sections are compared with next-to-next-to-

leading-order QCD calculations using various PDF sets. A comparison of the differential cross sections shows 1–2σ deviations from the predictions obtained with many of the recent PDF sets.

These results provide the first measurement of $W^\pm$ and Z boson production cross sections at the centre-of-mass energy $\sqrt{s} = 5.02$ TeV and complement previous measurements at $\sqrt{s} = 7$, 8 and 13 TeV. They constitute a reference for measurements of $W^\pm$ and Z boson production in heavy-ion collisions collected at $\sqrt{s_{NN}} = 5.02$ TeV by the LHC experiments.

Data Availability Statement This manuscript has no associated data or the data will not be deposited. [Authors' comment: All ATLAS scientific output is published in journals, and preliminary results are made available in Conference Notes. All are openly available, without restriction on use by external parties beyond copyright law and the standard conditions agreed by CERN. Data associated with journal publications are also made available: tables and data from plots (e.g. cross section values, likelihood profiles, selection efficiencies, cross section limits, ...) are stored in appropriate repositories such as HEPDATA (http://hepdata.cedar.ac.uk/). ATLAS also strives to make additional material related to the paper available that allows a reinterpretation of the data in the context of new theoretical models. For example, an extended encapsulation of the analysis is often provided for measurements in the framework of RIVET (http://rivet.hepforge.org/). This information is taken from the ATLAS Data Access Policy which is a public document that can be downloaded from http://opendata.cern.ch/record/413 [opendata.cern.ch].]

References

1. C. Anastasiou, L. Dixon, K. Melnikov, F. Petriello, High-precision QCD at hadron colliders: electroweak gauge boson rapidity distributions at next-to-next-to-leading order. Phys. Rev. D **69**, 094008 (2004). arXiv:hep-ph/0312266
2. S. Catani, M. Grazzini, Next-to-next-to-leading order subtraction formalism in hadron collisions and its application to Higgs boson production at the large hadron collider. Phys. Rev. Lett. **98**, 222002 (2007). arXiv:hep-ph/0703012
3. S. Catani, L. Cieri, G. Ferrera, D. de Florian, M. Grazzini, Vector boson production at hadron colliders: a fully exclusive QCD calculation at next-to-next-to-leading order. Phys. Rev. Lett. **103**, 082001 (2009). arXiv:0903.2120 [hep-ph]
4. ATLAS Collaboration, Precision measurement and interpretation of inclusive W^+, W^- and Z/γ^* production cross sections with the ATLAS detector. Eur. Phys. J. C **77**, 367 (2017). arXiv:1612.03016 [hep-ex]
5. ATLAS Collaboration, Measurement of $W^\pm$ and Z-boson production cross sections in pp collisions at $\sqrt{s} = 13$ TeV with the ATLAS detector. Phys. Lett. B **759**, 601 (2016). arXiv:1603.09222 [hep-ex]
6. CMS Collaboration, Measurement of inclusive W and Z boson production cross sections in pp collisions at $\sqrt{s} = 8$ TeV. Phys. Rev. Lett. **112**, 191802 (2014). arXiv:1402.0923 [hep-ex]
7. LHCb Collaboration, Measurement of forward W and Z boson production in pp collisions at $\sqrt{s} = 8$ TeV. JHEP **01**, 155 (2016). arXiv:1511.08039 [hep-ex]
8. ATLAS Collaboration, Measurement of the production and lepton charge asymmetry of W bosons in Pb+Pb collisions at $\sqrt{s_{NN}} = 2.76$ TeV with the ATLAS detector. Eur. Phys. J. C **75**, 23 (2015). arXiv:1408.4674 [hep-ex]
9. ATLAS Collaboration, Measurement of Z boson production in Pb-Pb collisions at $\sqrt{s_{NN}} = 2.76$ TeV with the ATLAS detector. Phys. Rev. Lett. **110**, 022301 (2013). arXiv:1210.6486 [hep-ex]
10. CMS Collaboration, Study of W boson production in PbPb and pp collisions at $\sqrt{s_{NN}} = 2.76$ TeV. Phys. Lett. B **715**, 66 (2012). arXiv:1205.6334 [nucl-ex]
11. CMS Collaboration, Study of Z production in PbPb and pp collisions at $\sqrt{s_{NN}} = 2.76$ TeV in the dimuon and dielectron decay channels. JHEP **03**, 022 (2015). arXiv:1410.4825 [nucl-ex]
12. ATLAS Collaboration, Z boson production in $p + Pb$ collisions at $\sqrt{s_{NN}} = 5.02$ TeV measured with the ATLAS detector. Phys. Rev. C **92**, 044915 (2015). arXiv:1507.06232 [hep-ex]
13. CMS Collaboration, Study of Z boson production in pPb collisions at $\sqrt{s_{NN}} = 5.02$ TeV. Phys. Lett. B **759**, 36 (2016). arXiv:1512.06461 [hep-ex]
14. ATLAS Collaboration, The ATLAS experiment at the CERN large hadron collider. JINST **3**, S08003 (2008)
15. ATLAS Collaboration, Performance of the ATLAS trigger system in 2015. Eur. Phys. J. C **77**, 317 (2017). arXiv:1611.09661 [hep-ex]
16. S. Agostinelli et al., GEANT4—a simulation toolkit. Nucl. Instrum. Methods A **506**, 250 (2003)
17. ATLAS Collaboration, The ATLAS simulation infrastructure. Eur. Phys. J. C **70**, 823 (2010). arXiv:1005.4568 [hep-ex]
18. S. Alioli, P. Nason, C. Oleari, E. Re, A general framework for implementing NLO calculations in shower Monte Carlo programs: the POWHEG BOX. JHEP **06**, 043 (2010). arXiv:1002.2581 [hep-ph]
19. T. Sjöstrand, S. Mrenna, P. Skands, A brief introduction to PYTHIA 8.1. Comput. Phys. Commun. **178**, 852 (2008). arXiv:0710.3820 [hep-ph]
20. J. Gao, CT10 next-to-next-to-leading order global analysis of QCD. Phys. Rev. D **89**, 033009 (2014). arXiv:1302.6246 [hep-ph]

21. J. Pumplin et al., New generation of parton distributions with uncertainties from global QCD analysis. JHEP **07**, 012 (2002). arXiv:hep-ph/0201195

22. ATLAS Collaboration, Measurement of the Z/γ^* boson transverse momentum distribution in pp collisions at $\sqrt{s} = 7$ TeV with the ATLAS detector. JHEP **09**, 145 (2014). arXiv:1406.3660 [hep-ex]

23. N. Davidson, T. Przedzinski, Z. Was, PHOTOS interface in C++: technical and physics documentation. Comput. Phys. Commun. **199**, 86 (2016). arXiv:1011.0937 [hep-ph]

24. H.-L. Lai et al., New parton distributions for collider physics. Phys. Rev. D **82**, 074024 (2010). arXiv:1007.2241 [hep-ph]

25. T. Sjöstrand, S. Mrenna, P. Skands, PYTHIA 6.4 physics and manual. JHEP **05**, 026 (2006). arXiv:hep-ph/0603175

26. P.Z. Skands, Tuning Monte Carlo generators: the Perugia tunes. Phys. Rev. D **82**, 074018 (2010). arXiv:1005.3457 [hep-ph]

27. D.J. Lange, The EvtGen particle decay simulation package. Nucl. Instrum. Methods A **462**, 152 (2001)

28. T. Gleisberg et al., Event generation with SHERPA 1.1. JHEP **02**, 007 (2009). arXiv:0811.4622 [hep-ph]

29. W.F.L. Hollik, Radiative corrections in the standard model and their rôle for precision tests of the electroweak theory. Fortsch. Phys. **38**, 165 (1990)

30. ATLAS Collaboration, Summary of ATLAS Pythia 8 tunes. ATL-PHYS-PUB-2012-003. https://cds.cern.ch/record/1474107

31. A.D. Martin, W.J. Stirling, R.S. Thorne, G. Watt, Parton distributions for the LHC. Eur. Phys. J. C **63**, 189 (2009). arXiv:0901.0002 [hep-ph]

32. ATLAS Collaboration, Electron efficiency measurements with the ATLAS detector using 2012 LHC proton-proton collision data. Eur. Phys. J. C **77**, 195 (2017). arXiv:1612.01456 [hep-ex]

33. ATLAS Collaboration, Electron efficiency measurements with the ATLAS detector using the 2015 LHC proton-proton collision data. ATLAS-CONF-2016-024. https://cds.cern.ch/record/2157687

34. ATLAS Collaboration, Muon reconstruction performance of the ATLAS detector in proton-proton collision data at $\sqrt{s} = 13$ TeV. Eur. Phys. J. C **76**, 292 (2016). arXiv:1603.05598 [hep-ex]

35. ATLAS Collaboration, Measurement of the W-boson mass in pp collisions at $\sqrt{s} = 7$ TeV with the ATLAS detector. Eur. Phys. J. C **78**,110 (2018). arXiv:1701.07240 [hep-ex]

36. ATLAS Collaboration, Topological cell clustering in the ATLAS calorimeters and its performance in LHC Run 1. Eur. Phys. J. C **77** 490 (2017). arXiv:1603.02934 [hep-ex]

37. ATLAS Collaboration, Jet reconstruction and performance using particle flow with the ATLAS detector. Eur. Phys. J. C **77**, 466 (2017). arXiv:1703.10485 [hep-ex]

38. ATLAS Collaboration, Electron and photon energy calibration with the ATLAS detector using LHC run 1 data. Eur. Phys. J. C **74**, 3071 (2014). arXiv:1407.5063 [hep-ex]

39. H. Abreu et al., Performance of the electronic readout of the ATLAS liquid argon calorimeters. JINST **5**, P09003 (2010)

40. ATLAS Collaboration, Luminosity determination in pp collisions at $\sqrt{s} = 8$ TeV using the ATLAS detector at the LHC. Eur. Phys. J. C **76**, 653 (2016). arXiv:1608.03953 [hep-ex]

41. G. Avoni et al., The new LUCID-2 detector for luminosity measurement and monitoring in ATLAS. JINST **13**, P07017 (2018)

42. E. Maguire, L. Heinrich, G. Watt, HEPData: a repository for high energy physics data. J. Phys. Conf. Ser. **898**, 102006 (2017). arXiv:1704.05473 [hep-ex]

43. A. Valassi, Combining correlated measurements of several different physical quantities. Nucl. Instrum. Methods A **500**, 391 (2003)

44. Particle Data Group, K.A. Olive et al., Review of particle physics. Chin. Phys. C **38**, 090001 (2014)

45. S. Dulat et al., New parton distribution functions from a global analysis of quantum chromodynamics. Phys. Rev. D **93**, 033006 (2016). arXiv:1506.07443 [hep-ph]

46. R.D. Ball et al., Parton distributions from high-precision collider data. Eur. Phys. J. C **77**, 663 (2017). arXiv:1706.00428 [hep-ph]

47. L.A. Harland-Lang, A.D. Martin, P. Motylinski, R.S. Thorne, Parton distributions in the LHC era: MMHT 2014 PDFs. Eur. Phys. J. C **75**, 204 (2015). arXiv:1412.3989 [hep-ph]

48. H1 and ZEUS Collaborations, Combination of measurements of inclusive deep inelastic $e^{\pm}p$ scattering cross sections and QCD analysis of HERA data. Eur. Phys. J. C **75**, 580 (2015). arXiv:1506.06042 [hep-ex]

49. S. Alekhin, J. Blümlein, S. Moch, R. Plačakytė, Parton distribution functions, α_s, and heavy-quark masses for LHC Run II. Phys. Rev. D **96**, 014011 (2017). arXiv:1701.05838 [hep-ph]

50. ATLAS Collaboration, Measurements of top-quark pair to Z-boson cross-section ratios at $\sqrt{s} = 13, 8, 7$ TeV with the ATLAS detector. JHEP **02**, 117 (2017). arXiv:1612.03636 [hep-ex]

51. E. Todesco, J. Wenninger, Large hadron collider momentum calibration and accuracy. Phys. Rev. Accel. Beams **20**, 081003 (2017)

52. ATLAS Collaboration, ATLAS Computing Acknowledgements. ATL-GEN-PUB-2016-002. https://cds.cern.ch/record/2202407

ATLAS Collaboration

M. Aaboud[34d],   G. Aad[99],   B. Abbott[125],   O. Abdinov[13,*],   B. Abeloos[129],   D. K. Abhayasinghe[91],   S. H. Abidi[164], O. S. AbouZeid[39], N. L. Abraham[153], H. Abramowicz[158], H. Abreu[157], Y. Abulaiti[6], B. S. Acharya[64a,64b,p], S. Adachi[160], L. Adamczyk[81a],   J. Adelman[119],   M. Adersberger[112],   A. Adiguzel[12c,aj],   T. Adye[141],   A. A. Affolder[143],   Y. Afik[157], C. Agheorghiesei[27c], J. A. Aguilar-Saavedra[137a,137f,ai], F. Ahmadov[77,ag], G. Aielli[71a,71b], S. Akatsuka[83], T. P. A. Åkesson[94], E. Akilli[52],   A. V. Akimov[108],   G. L. Alberghi[23a,23b],   J. Albert[173],   P. Albicocco[49],   M. J. Alconada Verzini[86], S. Alderweireldt[117],   M. Aleksa[35],   I. N. Aleksandrov[77],   C. Alexa[27b],   T. Alexopoulos[10],   M. Alhroob[125],   B. Ali[139], G. Alimonti[66a],   J. Alison[36],   S. P. Alkire[145],   C. Allaire[129],   B. M. M. Allbrooke[153],   B. W. Allen[128],   P. P. Allport[21], A. Aloisio[67a,67b],   A. Alonso[39],   F. Alonso[86],   C. Alpigiani[145],   A. A. Alshehri[55],   M. I. Alstaty[99],   B. Alvarez Gonzalez[35], D. Álvarez Piqueras[171],   M. G. Alviggi[67a,67b],   B. T. Amadio[18],   Y. Amaral Coutinho[78b],   L. Ambroz[132],   C. Amelung[26], D. Amidei[103],   S. P. Amor Dos Santos[137a,137c],   S. Amoroso[44],   C. S. Amrouche[52],   C. Anastopoulos[146],   L. S. Ancu[52], N. Andari[142],   T. Andeen[11],   C. F. Anders[59b],   J. K. Anders[20],   K. J. Anderson[36],   A. Andreazza[66a,66b],   V. Andrei[59a], C. R. Anelli[173], S. Angelidakis[37], I. Angelozzi[118], A. Angerami[38], A. V. Anisenkov[120a,120b], A. Annovi[69a], C. Antel[59a], M. T. Anthony[146], M. Antonelli[49], D. J. A. Antrim[168], F. Anulli[70a], M. Aoki[79], J. A. Aparisi Pozo[171], L. Aperio Bella[35], G. Arabidze[104], J. P. Araque[137a], V. Araujo Ferraz[78b], R. Araujo Pereira[78b], A. T. H. Arce[47], R. E. Ardell[91], F. A. Arduh[86], J.-F. Arguin[107],   S. Argyropoulos[75],   A. J. Armbruster[35],   L. J. Armitage[90],   A. Armstrong[168],   O. Arnaez[164],   H. Arnold[118],

M. Arratia[31], O. Arslan[24], A. Artamonov[109,*], G. Artoni[132], S. Artz[97], S. Asai[160], N. Asbah[57], E. M. Asimakopoulou[169], L. Asquith[153], K. Assamagan[29], R. Astalos[28a], R. J. Atkin[32a], M. Atkinson[170], N. B. Atlay[148], K. Augsten[139], G. Avolio[35], R. Avramidou[58a], M. K. Ayoub[15a], G. Azuelos[107,av], A. E. Baas[59a], M. J. Baca[21], H. Bachacou[142], K. Bachas[65a,65b], M. Backes[132], P. Bagnaia[70a,70b], M. Bahmani[82], H. Bahrasemani[149], A. J. Bailey[171], J. T. Baines[141], M. Bajic[39], C. Bakalis[10], O. K. Baker[180], P. J. Bakker[118], D. Bakshi Gupta[93], E. M. Baldin[120a,120b], P. Balek[177], F. Balli[142], W. K. Balunas[134], J. Balz[97], E. Banas[82], A. Bandyopadhyay[24], S. Banerjee[178,l], A. A. E. Bannoura[179], L. Barak[158], W. M. Barbe[37], E. L. Barberio[102], D. Barberis[53a,53b], M. Barbero[99], T. Barillari[113], M.-S. Barisits[35], J. Barkeloo[128], T. Barklow[150], R. Barnea[157], S. L. Barnes[58c], B. M. Barnett[141], R. M. Barnett[18], Z. Barnovska-Blenessy[58a], A. Baroncelli[72a], G. Barone[26], A. J. Barr[132], L. Barranco Navarro[171], F. Barreiro[96], J. Barreiro Guimarães da Costa[15a], R. Bartoldus[150], A. E. Barton[87], P. Bartos[28a], A. Basalaev[135], A. Bassalat[129], R. L. Bates[55], S. J. Batista[164], S. Batlamous[34e], J. R. Batley[31], M. Battaglia[143], M. Bauce[70a,70b], F. Bauer[142], K. T. Bauer[168], H. S. Bawa[150,n], J. B. Beacham[123], T. Beau[133], P. H. Beauchemin[167], P. Bechtle[24], H. C. Beck[51], H. P. Beck[20,s], K. Becker[50], M. Becker[97], C. Becot[44], A. Beddall[12d], A. J. Beddall[12a], V. A. Bednyakov[77], M. Bedognetti[118], C. P. Bee[152], T. A. Beermann[35], M. Begalli[78b], M. Begel[29], A. Behera[152], J. K. Behr[44], A. S. Bell[92], G. Bella[158], L. Bellagamba[23b], A. Bellerive[33], M. Bellomo[157], P. Bellos[9], K. Belotskiy[110], N. L. Belyaev[110], O. Benary[158,*], D. Benchekroun[34a], M. Bender[112], N. Benekos[10], Y. Benhammou[158], E. Benhar Noccioli[180], J. Benitez[75], D. P. Benjamin[47], M. Benoit[52], J. R. Bensinger[26], S. Bentvelsen[118], L. Beresford[132], M. Beretta[49], D. Berge[44], E. Bergeaas Kuutmann[169], N. Berger[5], L. J. Bergsten[26], J. Beringer[18], S. Berlendis[7], N. R. Bernard[100], G. Bernardi[133], C. Bernius[150], F. U. Bernlochner[24], T. Berry[91], P. Berta[97], C. Bertella[15a], G. Bertoli[43a,43b], I. A. Bertram[87], G. J. Besjes[39], O. Bessidskaia Bylund[179], M. Bessner[44], N. Besson[142], A. Bethani[98], S. Bethke[113], A. Betti[24], A. J. Bevan[90], J. Beyer[113], R. M. Bianchi[136], O. Biebel[112], D. Biedermann[19], R. Bielski[35], K. Bierwagen[97], N. V. Biesuz[69a,69b], M. Biglietti[72a], T. R. V. Billoud[107], M. Bindi[51], A. Bingul[12d], C. Bini[70a,70b], S. Biondi[23a,23b], M. Birman[177], T. Bisanz[51], J. P. Biswal[158], C. Bittrich[46], D. M. Bjergaard[47], J. E. Black[150], K. M. Black[25], T. Blazek[28a], I. Bloch[44], C. Blocker[26], A. Blue[55], U. Blumenschein[90], Dr. Blunier[144a], G. J. Bobbink[118], V. S. Bobrovnikov[120a,120b], S. S. Bocchetta[94], A. Bocci[47], D. Boerner[179], D. Bogavac[112], A. G. Bogdanchikov[120a,120b], C. Bohm[43a], V. Boisvert[91], P. Bokan[169], T. Bold[81a], A. S. Boldyrev[111], A. E. Bolz[59b], M. Bomben[133], M. Bona[90], J. S. Bonilla[128], M. Boonekamp[142], A. Borisov[121], G. Borissov[87], J. Bortfeldt[35], D. Bortoletto[132], V. Bortolotto[71a,71b], D. Boscherini[23b], M. Bosman[14], J. D. Bossio Sola[30], K. Bouaouda[34a], J. Boudreau[136], E. V. Bouhova-Thacker[87], D. Boumediene[37], C. Bourdarios[129], S. K. Boutle[55], A. Boveia[123], J. Boyd[35], D. Boye[32b], I. R. Boyko[77], A. J. Bozson[91], J. Bracinik[21], N. Brahimi[99], A. Brandt[8], G. Brandt[179], O. Brandt[59a], F. Braren[44], U. Bratzler[161], B. Brau[100], J. E. Brau[128], W. D. Breaden Madden[55], K. Brendlinger[44], L. Brenner[44], R. Brenner[169], S. Bressler[177], B. Brickwedde[97], D. L. Briglin[21], D. Britton[55], D. Britzger[59b], I. Brock[24], R. Brock[104], G. Brooijmans[38], T. Brooks[91], W. K. Brooks[144b], E. Brost[119], J. H Broughton[21], P. A. Bruckman de Renstrom[82], D. Bruncko[28b], A. Bruni[23b], G. Bruni[23b], L. S. Bruni[118], S. Bruno[71a,71b], B.H. Brunt[31], M. Bruschi[23b], N. Bruscino[136], P. Bryant[36], L. Bryngemark[44], T. Buanes[17], Q. Buat[35], P. Buchholz[148], A. G. Buckley[55], I. A. Budagov[77], M. K. Bugge[131], F. Bührer[50], O. Bulekov[110], D. Bullock[8], T. J. Burch[119], S. Burdin[88], C. D. Burgard[118], A. M. Burger[5], B. Burghgrave[119], K. Burka[82], S. Burke[141], I. Burmeister[45], J. T. P. Burr[132], V. Büscher[97], E. Buschmann[51], P. Bussey[55], J. M. Butler[25], C. M. Buttar[55], J. M. Butterworth[92], P. Butti[35], W. Buttinger[35], A. Buzatu[155], A. R. Buzykaev[120a,120b], G. Cabras[23a,23b], S. Cabrera Urbán[171], D. Caforio[139], H. Cai[170], V. M. M. Cairo[2], O. Cakir[4a], N. Calace[52], P. Calafiura[18], A. Calandri[99], G. Calderini[133], P. Calfayan[63], G. Callea[40a,40b], L. P. Caloba[78b], S. Calvente Lopez[96], D. Calvet[37], S. Calvet[37], T. P. Calvet[152], M. Calvetti[69a,69b], R. Camacho Toro[133], S. Camarda[35], P. Camarri[71a,71b], D. Cameron[131], R. Caminal Armadans[100], C. Camincher[35], S. Campana[35], M. Campanelli[92], A. Camplani[39], A. Campoverde[148], V. Canale[67a,67b], M. Cano Bret[58c], J. Cantero[126], T. Cao[158], Y. Cao[170], M. D. M. Capeans Garrido[35], I. Caprini[27b], M. Caprini[27b], M. Capua[40a,40b], R. M. Carbone[38], R. Cardarelli[71a], F. C. Cardillo[146], I. Carli[140], T. Carli[35], G. Carlino[67a], B. T. Carlson[136], L. Carminati[66a,66b], R. M. D. Carney[43a,43b], S. Caron[117], E. Carquin[144b], S. Carrá[66a,66b], G. D. Carrillo-Montoya[35], D. Casadei[32b], M. P. Casado[14,g], A. F. Casha[164], D. W. Casper[168], R. Castelijn[118], R. Castillo[171], V. Castillo Gimenez[171], N. F. Castro[137a,137e], A. Catinaccio[35], J. R. Catmore[131], A. Cattai[35], J. Caudron[24], V. Cavaliere[29], E. Cavallaro[14], D. Cavalli[66a], M. Cavalli-Sforza[14], V. Cavasinni[69a,69b], E. Celebi[12b], F. Ceradini[72a,72b], L. Cerda Alberich[171], A. S. Cerqueira[78a], A. Cerri[153], L. Cerrito[71a,71b], F. Cerutti[18], A. Cervelli[23a,23b], S. A. Cetin[12b], A. Chafaq[34a], D. Chakraborty[119], S. K. Chan[57], W. S. Chan[118], Y. L. Chan[61a], J. D. Chapman[31], B. Chargeishvili[156b], D. G. Charlton[21], C. C. Chau[33], C. A. Chavez Barajas[153], S. Che[123], A. Chegwidden[104], S. Chekanov[6], S. V. Chekulaev[165a], G. A. Chelkov[77,au], M. A. Chelstowska[35], C. Chen[58a], C. H. Chen[76], H. Chen[29], J. Chen[58a], J. Chen[38], S. Chen[134], S. J. Chen[15c], X. Chen[15b,at], Y. Chen[80], Y.-H. Chen[44], H. C. Cheng[103], H. J. Cheng[15d], A. Cheplakov[77], E. Cheremushkina[121], R. Cherkaoui El Moursli[34e], E. Cheu[7], K. Cheung[62], L. Chevalier[142], V. Chiarella[49], G. Chiarelli[69a], G. Chiodini[65a], A. S. Chisholm[35,21], A. Chitan[27b], I. Chiu[160],

Y. H. Chiu[173], M. V. Chizhov[77], K. Choi[63], A. R. Chomont[129], S. Chouridou[159], Y. S. Chow[118], V. Christodoulou[92], M. C. Chu[61a], J. Chudoba[138], A. J. Chuinard[101], J. J. Chwastowski[82], L. Chytka[127], D. Cinca[45], V. Cindro[89], I. A. Cioară[24], A. Ciocio[18], F. Cirotto[67a,67b], Z. H. Citron[177], M. Citterio[66a], A. Clark[52], M. R. Clark[38], P. J. Clark[48], C. Clement[43a,43b], Y. Coadou[99], M. Cobal[64a,64c], A. Coccaro[53a,53b], J. Cochran[76], H. Cohen[158], A. E. C. Coimbra[177], L. Colasurdo[117], B. Cole[38], A. P. Colijn[118], J. Collot[56], P. Conde Muiño[137a,i], E. Coniavitis[50], S. H. Connell[32b], I. A. Connelly[98], S. Constantinescu[27b], F. Conventi[67a,aw], A. M. Cooper-Sarkar[132], F. Cormier[172], K. J. R. Cormier[164], L. D. Corpe[92], M. Corradi[70a,70b], E. E. Corrigan[94], F. Corriveau[101,ae], A. Cortes-Gonzalez[35], M. J. Costa[171], F. Costanza[5], D. Costanzo[146], G. Cottin[31], G. Cowan[91], B. E. Cox[98], J. Crane[98], K. Cranmer[122], S. J. Crawley[55], R. A. Creager[134], G. Cree[33], S. Crépé-Renaudin[56], F. Crescioli[133], M. Cristinziani[24], V. Croft[122], G. Crosetti[40a,40b], A. Cueto[96], T. Cuhadar Donszelmann[146], A. R. Cukierman[150], S. Czekierda[82], P. Czodrowski[35], M. J. Da Cunha Sargedas De Sousa[58b], C. Da Via[98], W. Dabrowski[81a], T. Dado[28a,z], S. Dahbi[34e], T. Dai[103], F. Dallaire[107], C. Dallapiccola[100], M. Dam[39], G. D'amen[23a,23b], J. Damp[97], J. R. Dandoy[134], M. F. Daneri[30], N. P. Dang[178,l], N. D. Dann[98], M. Danninger[172], V. Dao[35], G. Darbo[53b], S. Darmora[8], O. Dartsi[5], A. Dattagupta[128], T. Daubney[44], S. D'Auria[55], W. Davey[24], C. David[44], T. Davidek[140], D. R. Davis[47], E. Dawe[102], I. Dawson[146], K. De[8], R. De Asmundis[67a], A. De Benedetti[125], M. De Beurs[118], S. De Castro[23a,23b], S. De Cecco[70a,70b], N. De Groot[117], P. de Jong[118], H. De la Torre[104], F. De Lorenzi[76], A. De Maria[51,u], D. De Pedis[70a], A. De Salvo[70a], U. De Sanctis[71a,71b], M. De Santis[71a,71b], A. De Santo[153], K. De Vasconcelos Corga[99], J. B. De Vivie De Regie[129], C. Debenedetti[143], D. V. Dedovich[77], N. Dehghanian[3], M. Del Gaudio[40a,40b], J. Del Peso[96], Y. Delabat Diaz[44], D. Delgove[129], F. Deliot[142], C. M. Delitzsch[7], M. Della Pietra[67a,67b], D. Della Volpe[52], A. Dell'Acqua[35], L. Dell'Asta[25], M. Delmastro[5], C. Delporte[129], P. A. Delsart[56], D. A. DeMarco[164], S. Demers[180], M. Demichev[77], S. P. Denisov[121], D. Denysiuk[118], L. D'Eramo[133], D. Derendarz[82], J. E. Derkaoui[34d], F. Derue[133], P. Dervan[88], K. Desch[24], C. Deterre[44], K. Dette[164], M. R. Devesa[30], P. O. Deviveiros[35], A. Dewhurst[141], S. Dhaliwal[26], F. A. Di Bello[52], A. Di Ciaccio[71a,71b], L. Di Ciaccio[5], W. K. Di Clemente[134], C. Di Donato[67a,67b], A. Di Girolamo[35], B. Di Micco[72a,72b], R. Di Nardo[100], K. F. Di Petrillo[57], R. Di Sipio[164], D. Di Valentino[33], C. Diaconu[99], M. Diamond[164], F. A. Dias[39], T. Dias Do Vale[137a], M. A. Diaz[144a], J. Dickinson[18], E. B. Diehl[103], J. Dietrich[19], S. Díez Cornell[44], A. Dimitrievska[18], J. Dingfelder[24], F. Dittus[35], F. Djama[99], T. Djobava[156b], J. I. Djuvsland[59a], M. A. B. Do Vale[78c], M. Dobre[27b], D. Dodsworth[26], C. Doglioni[94], J. Dolejsi[140], Z. Dolezal[140], M. Donadelli[78d], J. Donini[37], A. D'onofrio[90], M. D'Onofrio[88], J. Dopke[141], A. Doria[67a], M. T. Dova[86], A. T. Doyle[55], E. Drechsler[51], E. Dreyer[149], T. Dreyer[51], Y. Du[58b], F. Dubinin[108], M. Dubovsky[28a], A. Dubreuil[52], E. Duchovni[177], G. Duckeck[112], A. Ducourthial[133], O. A. Ducu[107,y], D. Duda[113], A. Dudarev[35], A. C. Dudder[97], E. M. Duffield[18], L. Duflot[129], M. Dührssen[35], C. Dülsen[179], M. Dumancic[177], A. E. Dumitriu[27b,e], A. K. Duncan[55], M. Dunford[59a], A. Duperrin[99], H. Duran Yildiz[4a], M. Düren[54], A. Durglishvili[156b], D. Duschinger[46], B. Dutta[44], D. Duvnjak[1], M. Dyndal[44], S. Dysch[98], B. S. Dziedzic[82], C. Eckardt[44], K. M. Ecker[113], R. C. Edgar[103], T. Eifert[35], G. Eigen[17], K. Einsweiler[18], T. Ekelof[169], M. El Kacimi[34c], R. El Kosseifi[99], V. Ellajosyula[99], M. Ellert[169], F. Ellinghaus[179], A. A. Elliot[90], N. Ellis[35], J. Elmsheuser[29], M. Elsing[35], D. Emeliyanov[141], Y. Enari[160], J. S. Ennis[175], M. B. Epland[47], J. Erdmann[45], A. Ereditato[20], S. Errede[170], M. Escalier[129], C. Escobar[171], O. Estrada Pastor[171], A. I. Etienvre[142], E. Etzion[158], H. Evans[63], A. Ezhilov[135], M. Ezzi[34e], F. Fabbri[55], L. Fabbri[23a,23b], V. Fabiani[117], G. Facini[92], R. M. Faisca Rodrigues Pereira[137a], R. M. Fakhrutdinov[121], S. Falciano[70a], P. J. Falke[5], S. Falke[5], J. Faltova[140], Y. Fang[15a], M. Fanti[66a,66b], A. Farbin[8], A. Farilla[72a], E. M. Farina[68a,68b], T. Farooque[104], S. Farrell[18], S. M. Farrington[175], P. Farthouat[35], F. Fassi[34e], P. Fassnacht[35], D. Fassouliotis[9], M. Faucci Giannelli[48], A. Favareto[53a,53b], W. J. Fawcett[31], L. Fayard[129], O. L. Fedin[135,q], W. Fedorko[172], M. Feickert[41], S. Feigl[131], L. Feligioni[99], C. Feng[58b], E. J. Feng[35], M. Feng[47], M. J. Fenton[55], A. B. Fenyuk[121], L. Feremenga[8], J. Ferrando[44], A. Ferrari[169], P. Ferrari[118], R. Ferrari[68a], D. E. Ferreira de Lima[59b], A. Ferrer[171], D. Ferrere[52], C. Ferretti[103], F. Fiedler[97], A. Filipčič[89], F. Filthaut[117], K. D. Finelli[25], M. C. N. Fiolhais[137a,137c,a], L. Fiorini[171], C. Fischer[14], W. C. Fisher[104], N. Flaschel[44], I. Fleck[148], P. Fleischmann[103], R. R. M. Fletcher[134], T. Flick[179], B. M. Flierl[112], L. M. Flores[134], L. R. Flores Castillo[61a], F. M. Follega[73a,73b], N. Fomin[17], G. T. Forcolin[98], A. Formica[142], F. A. Förster[14], A. C. Forti[98], A. G. Foster[21], D. Fournier[129], H. Fox[87], S. Fracchia[146], P. Francavilla[69a,69b], M. Franchini[23a,23b], S. Franchino[59a], D. Francis[35], L. Franconi[131], M. Franklin[57], M. Frate[168], M. Fraternali[68a,68b], A. N. Fray[90], D. Freeborn[92], S. M. Fressard-Batraneanu[35], B. Freund[107], W. S. Freund[78b], D. C. Frizzell[125], D. Froidevaux[35], J. A. Frost[132], C. Fukunaga[161], E. Fullana Torregrosa[171], T. Fusayasu[114], J. Fuster[171], O. Gabizon[157], A. Gabrielli[23a,23b], A. Gabrielli[18], G. P. Gach[81a], S. Gadatsch[52], P. Gadow[113], G. Gagliardi[53a,53b], L. G. Gagnon[107], C. Galea[27b], B. Galhardo[137a,137c], E. J. Gallas[132], B. J. Gallop[141], P. Gallus[139], G. Galster[39], R. Gamboa Goni[90], K. K. Gan[123], S. Ganguly[177], J. Gao[58a], Y. Gao[88], Y. S. Gao[150,n], C. García[171], J. E. García Navarro[171], J. A. García Pascual[15a], M. Garcia-Sciveres[18], R. W. Gardner[36], N. Garelli[150], V. Garonne[131], K. Gasnikova[44], A. Gaudiello[53a,53b], G. Gaudio[68a], I. L. Gavrilenko[108], A. Gavrilyuk[109], C. Gay[172], G. Gaycken[24], E. N. Gazis[10], C. N. P. Gee[141], J. Geisen[51], M. Geisen[97], M. P. Geisler[59a], K. Gellerstedt[43a,43b],

C. Gemme[53b], M. H. Genest[56], C. Geng[103], S. Gentile[70a,70b], S. George[91], D. Gerbaudo[14], G. Gessner[45], S. Ghasemi[148], M. Ghasemi Bostanabad[173], M. Ghneimat[24], B. Giacobbe[23b], S. Giagu[70a,70b], N. Giangiacomi[23a,23b], P. Giannetti[69a], A. Giannini[67a,67b], S. M. Gibson[91], M. Gignac[143], D. Gillberg[33], G. Gilles[179], D. M. Gingrich[3,av], M. P. Giordani[64a,64c], F. M. Giorgi[23b], P. F. Giraud[142], P. Giromini[57], G. Giugliarelli[64a,64c], D. Giugni[66a], F. Giuli[132], M. Giulini[59b], S. Gkaitatzis[159], I. Gkialas[9,k], E. L. Gkougkousis[14], P. Gkountoumis[10], L. K. Gladilin[111], C. Glasman[96], J. Glatzer[14], P. C. F. Glaysher[44], A. Glazov[44], M. Goblirsch-Kolb[26], J. Godlewski[82], S. Goldfarb[102], T. Golling[52], D. Golubkov[121], A. Gomes[137a,137b], R. Goncalves Gama[78a], R. Gonçalo[137a], G. Gonella[50], L. Gonella[21], A. Gongadze[77], F. Gonnella[21], J. L. Gonski[57], S. González de la Hoz[171], S. Gonzalez-Sevilla[52], L. Goossens[35], P. A. Gorbounov[109], H. A. Gordon[29], B. Gorini[35], E. Gorini[65a,65b], A. Gorišek[89], A. T. Goshaw[47], C. Gössling[45], M. I. Gostkin[77], C. A. Gottardo[24], C. R. Goudet[129], D. Goujdami[34c], A. G. Goussiou[145], N. Govender[32b,c], C. Goy[5], E. Gozani[157], I. Grabowska-Bold[81a], P. O. J. Gradin[169], E. C. Graham[88], J. Gramling[168], E. Gramstad[131], S. Grancagnolo[19], V. Gratchev[135], P. M. Gravila[27f], F. G. Gravili[65a,65b], C. Gray[55], H. M. Gray[18], Z. D. Greenwood[93,al], C. Grefe[24], K. Gregersen[94], I. M. Gregor[44], P. Grenier[150], K. Grevtsov[44], N. A. Grieser[125], J. Griffiths[8], A. A. Grillo[143], K. Grimm[150,b], S. Grinstein[14,aa], Ph. Gris[37], J.-F. Grivaz[129], S. Groh[97], E. Gross[177], J. Grosse-Knetter[51], G. C. Grossi[93], Z. J. Grout[92], C. Grud[103], A. Grummer[116], L. Guan[103], W. Guan[178], J. Guenther[35], A. Guerguichon[129], F. Guescini[165a], D. Guest[168], R. Gugel[50], B. Gui[123], T. Guillemin[5], S. Guindon[35], U. Gul[55], C. Gumpert[35], J. Guo[58c], W. Guo[103], Y. Guo[58a,t], Z. Guo[99], R. Gupta[41], S. Gurbuz[12c], G. Gustavino[125], B. J. Gutelman[157], P. Gutierrez[125], C. Gutschow[92], C. Guyot[142], M. P. Guzik[81a], C. Gwenlan[132], C. B. Gwilliam[88], A. Haas[122], C. Haber[18], H. K. Hadavand[8], N. Haddad[34e], A. Hadef[58a], S. Hageböck[24], M. Hagihara[166], H. Hakobyan[181,*], M. Haleem[174], J. Haley[126], G. Halladjian[104], G. D. Hallewell[99], K. Hamacher[179], P. Hamal[127], K. Hamano[173], A. Hamilton[32a], G. N. Hamity[146], K. Han[58a,ak], L. Han[58a], S. Han[15d], K. Hanagaki[79,w], M. Hance[143], D. M. Handl[112], B. Haney[134], R. Hankache[133], P. Hanke[59a], E. Hansen[94], J. B. Hansen[39], J. D. Hansen[39], M. C. Hansen[24], P. H. Hansen[39], K. Hara[166], A. S. Hard[178], T. Harenberg[179], S. Harkusha[105], P. F. Harrison[175], N. M. Hartmann[112], Y. Hasegawa[147], A. Hasib[48], S. Hassani[142], S. Haug[20], R. Hauser[104], L. Hauswald[46], L. B. Havener[38], M. Havranek[139], C. M. Hawkes[21], R. J. Hawkings[35], D. Hayden[104], C. Hayes[152], C. P. Hays[132], J. M. Hays[90], H. S. Hayward[88], S. J. Haywood[141], M. P. Heath[48], V. Hedberg[94], L. Heelan[8], S. Heer[24], K. K. Heidegger[50], J. Heilman[33], S. Heim[44], T. Heim[18], B. Heinemann[44,aq], J. J. Heinrich[112], L. Heinrich[122], C. Heinz[54], J. Hejbal[138], L. Helary[35], A. Held[172], S. Hellesund[131], S. Hellman[43a,43b], C. Helsens[35], R. C. W. Henderson[87], Y. Heng[178], S. Henkelmann[172], A. M. Henriques Correia[35], G. H. Herbert[19], H. Herde[26], V. Herget[174], Y. Hernández Jiménez[32c], H. Herr[97], M. G. Herrmann[112], G. Herten[50], R. Hertenberger[112], L. Hervas[35], T. C. Herwig[134], G. G. Hesketh[92], N. P. Hessey[165a], J. W. Hetherly[41], S. Higashino[79], E. Higón-Rodriguez[171], K. Hildebrand[36], E. Hill[173], J. C. Hill[31], K. K. Hill[29], K. H. Hiller[44], S. J. Hillier[21], M. Hils[46], I. Hinchliffe[18], M. Hirose[130], D. Hirschbuehl[179], B. Hiti[89], O. Hladik[138], D. R. Hlaluku[32c], X. Hoad[48], J. Hobbs[152], N. Hod[165a], M. C. Hodgkinson[146], A. Hoecker[35], M. R. Hoeferkamp[116], F. Hoenig[112], D. Hohn[24], D. Hohov[129], T. R. Holmes[36], M. Holzbock[112], M. Homann[45], S. Honda[166], T. Honda[79], T. M. Hong[136], A. Hönle[113], B. H. Hooberman[170], W. H. Hopkins[128], Y. Horii[115], P. Horn[46], A. J. Horton[149], L. A. Horyn[36], J.-Y. Hostachy[56], A. Hostiuc[145], S. Hou[155], A. Hoummada[34a], J. Howarth[98], J. Hoya[86], M. Hrabovsky[127], I. Hristova[19], J. Hrivnac[129], A. Hrynevich[106], T. Hryn'ova[5], P. J. Hsu[62], S.-C. Hsu[145], Q. Hu[29], S. Hu[58c], Y. Huang[15a], Z. Hubacek[139], F. Hubaut[99], M. Huebner[24], F. Huegging[24], T. B. Huffman[132], E. W. Hughes[38], M. Huhtinen[35], R. F. H. Hunter[33], P. Huo[152], A. M. Hupe[33], N. Huseynov[77,ag], J. Huston[104], J. Huth[57], R. Hyneman[103], G. Iacobucci[52], G. Iakovidis[29], I. Ibragimov[148], L. Iconomidou-Fayard[129], Z. Idrissi[34e], P. Iengo[35], R. Ignazzi[39], O. Igonkina[118,ac], R. Iguchi[160], T. Iizawa[52], Y. Ikegami[79], M. Ikeno[79], D. Iliadis[159], N. Ilic[117], F. Iltzsche[46], G. Introzzi[68a,68b], M. Iodice[72a], K. Iordanidou[38], V. Ippolito[70a,70b], M. F. Isacson[169], N. Ishijima[130], M. Ishino[160], M. Ishitsuka[162], W. Islam[126], C. Issever[132], S. Istin[157], F. Ito[166], J. M. Iturbe Ponce[61a], R. Iuppa[73a,73b], A. Ivina[177], H. Iwasaki[79], J. M. Izen[42], V. Izzo[67a], P. Jacka[138], P. Jackson[1], R. M. Jacobs[24], V. Jain[2], G. Jäkel[179], K. B. Jakobi[97], K. Jakobs[50], S. Jakobsen[74], T. Jakoubek[138], D. O. Jamin[126], D. K. Jana[93], R. Jansky[52], J. Janssen[24], M. Janus[51], P. A. Janus[81a], G. Jarlskog[94], N. Javadov[77,ag], T. Javůrek[35], M. Javurkova[50], F. Jeanneau[142], L. Jeanty[18], J. Jejelava[156a,ah], A. Jelinskas[175], P. Jenni[50,d], J. Jeong[44], N. Jeong[44], S. Jézéquel[5], H. Ji[178], J. Jia[152], H. Jiang[76], Y. Jiang[58a], Z. Jiang[150,r], S. Jiggins[50], F. A. Jimenez Morales[37], J. Jimenez Pena[171], S. Jin[15c], A. Jinaru[27b], O. Jinnouchi[162], H. Jivan[32c], P. Johansson[146], K. A. Johns[7], C. A. Johnson[63], W. J. Johnson[145], K. Jon-And[43a,43b], R. W. L. Jones[87], S. D. Jones[153], S. Jones[7], T. J. Jones[88], J. Jongmanns[59a], P. M. Jorge[137a,137b], J. Jovicevic[165a], X. Ju[18], J. J. Junggeburth[113], A. Juste Rozas[14,aa], A. Kaczmarska[82], M. Kado[129], H. Kagan[123], M. Kagan[150], T. Kaji[176], E. Kajomovitz[157], C. W. Kalderon[94], A. Kaluza[97], S. Kama[41], A. Kamenshchikov[121], L. Kanjir[89], Y. Kano[160], V. A. Kantserov[110], J. Kanzaki[79], B. Kaplan[122], L. S. Kaplan[178], D. Kar[32c], M. J. Kareem[165b], E. Karentzos[10], S. N. Karpov[77], Z. M. Karpova[77], V. Kartvelishvili[87], A. N. Karyukhin[121], L. Kashif[178], R. D. Kass[123], A. Kastanas[151], Y. Kataoka[160], C. Kato[58c,58d], J. Katzy[44], K. Kawade[80], K. Kawagoe[85], T. Kawamoto[160], G. Kawamura[51],

E. F. Kay[88], V. F. Kazanin[120a,120b], R. Keeler[173], R. Kehoe[41], J. S. Keller[33], E. Kellermann[94], J. J. Kempster[21], J. Kendrick[21], O. Kepka[138], S. Kersten[179], B. P. Kerševan[89], R. A. Keyes[101], M. Khader[170], F. Khalil-Zada[13], A. Khanov[126], A. G. Kharlamov[120a,120b], T. Kharlamova[120a,120b], E. E. Khoda[172], A. Khodinov[163], T. J. Khoo[52], E. Khramov[77], J. Khubua[156b], S. Kido[80], M. Kiehn[52], C. R. Kilby[91], Y. K. Kim[36], N. Kimura[64a,64c], O. M. Kind[19], B. T. King[88], D. Kirchmeier[46], J. Kirk[141], A. E. Kiryunin[113], T. Kishimoto[160], D. Kisielewska[81a], V. Kitali[44], O. Kivernyk[5], E. Kladiva[28b,*], T. Klapdor-Kleingrothaus[50], M. H. Klein[103], M. Klein[88], U. Klein[88], K. Kleinknecht[97], P. Klimek[119], A. Klimentov[29], R. Klingenberg[45,*], T. Klingl[24], T. Klioutchnikova[35], F. F. Klitzner[112], P. Kluit[118], S. Kluth[113], E. Kneringer[74], E. B. F. G. Knoops[99], A. Knue[50], A. Kobayashi[160], D. Kobayashi[85], T. Kobayashi[160], M. Kobel[46], M. Kocian[150], P. Kodys[140], P. T. Koenig[24], T. Koffas[33], E. Koffeman[118], N. M. Köhler[113], T. Koi[150], M. Kolb[59b], I. Koletsou[5], T. Kondo[79], N. Kondrashova[58c], K. Köneke[50], A. C. König[117], T. Kono[79], R. Konoplich[122,an], V. Konstantinides[92], N. Konstantinidis[92], B. Konya[94], R. Kopeliansky[63], S. Koperny[81a], K. Korcyl[82], K. Kordas[159], G. Koren[158], A. Korn[92], I. Korolkov[14], E. V. Korolkova[146], N. Korotkova[111], O. Kortner[113], S. Kortner[113], T. Kosek[140], V. V. Kostyukhin[24], A. Kotwal[47], A. Koulouris[10], A. Kourkoumeli-Charalampidi[68a,68b], C. Kourkoumelis[9], E. Kourlitis[146], V. Kouskoura[29], A. B. Kowalewska[82], R. Kowalewski[173], T. Z. Kowalski[81a], C. Kozakai[160], W. Kozanecki[142], A. S. Kozhin[121], V. A. Kramarenko[111], G. Kramberger[89], D. Krasnopevtsev[58a], M. W. Krasny[133], A. Krasznahorkay[35], D. Krauss[113], J. A. Kremer[81a], J. Kretzschmar[88], P. Krieger[164], K. Krizka[18], K. Kroeninger[45], H. Kroha[113], J. Kroll[138], J. Kroll[134], J. Krstic[16], U. Kruchonak[77], H. Krüger[24], N. Krumnack[76], M. C. Kruse[47], T. Kubota[102], S. Kuday[4b], J. T. Kuechler[179], S. Kuehn[35], A. Kugel[59a], F. Kuger[174], T. Kuhl[44], V. Kukhtin[77], R. Kukla[99], Y. Kulchitsky[105], S. Kuleshov[144b], Y. P. Kulinich[170], M. Kuna[56], T. Kunigo[83], A. Kupco[138], T. Kupfer[45], O. Kuprash[158], H. Kurashige[80], L. L. Kurchaninov[165a], Y. A. Kurochkin[105], M. G. Kurth[15d], E. S. Kuwertz[35], M. Kuze[162], J. Kvita[127], T. Kwan[101], A. La Rosa[113], J. L. La Rosa Navarro[78d], L. La Rotonda[40a,40b], F. La Ruffa[40a,40b], C. Lacasta[171], F. Lacava[70a,70b], J. Lacey[44], D. P. J. Lack[98], H. Lacker[19], D. Lacour[133], E. Ladygin[77], R. Lafaye[5], B. Laforge[133], T. Lagouri[32c], S. Lai[51], S. Lammers[63], W. Lampl[7], E. Lançon[29], U. Landgraf[50], M. P. J. Landon[90], M. C. Lanfermann[52], V. S. Lang[44], J. C. Lange[14], R. J. Langenberg[35], A. J. Lankford[168], F. Lanni[29], K. Lantzsch[24], A. Lanza[68a], A. Lapertosa[53a,53b], S. Laplace[133], J. F. Laporte[142], T. Lari[66a], F. Lasagni Manghi[23a,23b], M. Lassnig[35], T. S. Lau[61a], A. Laudrain[129], M. Lavorgna[67a,67b], A. T. Law[143], M. Lazzaroni[66a,66b], B. Le[102], O. Le Dortz[133], E. Le Guirriec[99], E. P. Le Quilleuc[142], M. LeBlanc[7], T. LeCompte[6], F. Ledroit-Guillon[56], C. A. Lee[29], G. R. Lee[144a], L. Lee[57], S. C. Lee[155], B. Lefebvre[101], M. Lefebvre[173], F. Legger[112], C. Leggett[18], K. Lehmann[149], N. Lehmann[179], G. Lehmann Miotto[35], W. A. Leight[44], A. Leisos[159,x], M. A. L. Leite[78d], R. Leitner[140], D. Lellouch[177], B. Lemmer[51], K. J. C. Leney[92], T. Lenz[24], B. Lenzi[35], R. Leone[7], S. Leone[69a], C. Leonidopoulos[48], G. Lerner[153], C. Leroy[107], R. Les[164], A. A. J. Lesage[142], C. G. Lester[31], M. Levchenko[135], J. Levêque[5], D. Levin[103], L. J. Levinson[177], D. Lewis[90], B. Li[103], C.-Q. Li[58a,am], H. Li[58b], L. Li[58c], Q. Li[15d], Q. Y. Li[58a], S. Li[58c,58d], X. Li[58c], Y. Li[148], Z. Liang[15a], B. Liberti[71a], A. Liblong[164], K. Lie[61c], S. Liem[118], A. Limosani[154], C. Y. Lin[31], K. Lin[104], T. H. Lin[97], R. A. Linck[63], J. H. Lindon[21], B. E. Lindquist[152], A. L. Lionti[52], E. Lipeles[134], A. Lipniacka[17], M. Lisovyi[59b], T. M. Liss[170,as], A. Lister[172], A. M. Litke[143], J. D. Little[8], B. Liu[76], B. L Liu[6], H. B. Liu[29], H. Liu[103], J. B. Liu[58a], J. K. K. Liu[132], K. Liu[133], M. Liu[58a], P. Liu[18], Y. Liu[15a], Y. L. Liu[58a], Y. W. Liu[58a], M. Livan[68a,68b], A. Lleres[56], J. Llorente Merino[15a], S. L. Lloyd[90], C. Y. Lo[61b], F. Lo Sterzo[41], E. M. Lobodzinska[44], P. Loch[7], T. Lohse[19], K. Lohwasser[146], M. Lokajicek[138], B. A. Long[25], J. D. Long[170], R. E. Long[87], L. Longo[65a,65b], K. A. Looper[123], J. A. Lopez[144b], I. Lopez Paz[14], A. Lopez Solis[146], J. Lorenz[112], N. Lorenzo Martinez[5], M. Losada[22], P. J. Lösel[112], A. Lösle[50], X. Lou[44], X. Lou[15a], A. Lounis[129], J. Love[6], P. A. Love[87], J. J. Lozano Bahilo[171], H. Lu[61a], M. Lu[58a], N. Lu[103], Y. J. Lu[62], H. J. Lubatti[145], C. Luci[70a,70b], A. Lucotte[56], C. Luedtke[50], F. Luehring[63], I. Luise[133], L. Luminari[70a], B. Lund-Jensen[151], M. S. Lutz[100], P. M. Luzi[133], D. Lynn[29], R. Lysak[138], E. Lytken[94], F. Lyu[15a], V. Lyubushkin[77], H. Ma[29], L. L. Ma[58b], Y. Ma[58b], G. Maccarrone[49], A. Macchiolo[113], C. M. Macdonald[146], J. Machado Miguens[134,137b], D. Madaffari[171], R. Madar[37], W. F. Mader[46], A. Madsen[44], N. Madysa[46], J. Maeda[80], K. Maekawa[160], S. Maeland[17], T. Maeno[29], A. S. Maevskiy[111], V. Magerl[50], C. Maidantchik[78b], T. Maier[112], A. Maio[137a,137b,137d], O. Majersky[28a], S. Majewski[128], Y. Makida[79], N. Makovec[129], B. Malaescu[133], Pa. Malecki[82], V. P. Maleev[135], F. Malek[56], U. Mallik[75], D. Malon[6], C. Malone[31], S. Maltezos[10], S. Malyukov[35], J. Mamuzic[171], G. Mancini[49], I. Mandić[89], J. Maneira[137a], L. Manhaes de Andrade Filho[78a], J. Manjarres Ramos[46], K. H. Mankinen[94], A. Mann[112], A. Manousos[74], B. Mansoulie[142], J. D. Mansour[15a], M. Mantoani[51], S. Manzoni[66a,66b], G. Marceca[30], L. March[52], L. Marchese[132], G. Marchiori[133], M. Marcisovsky[138], C. A. Marin Tobon[35], M. Marjanovic[37], D. E. Marley[103], F. Marroquim[78b], Z. Marshall[18], M. U. F Martensson[169], S. Marti-Garcia[171], C. B. Martin[123], T. A. Martin[175], V. J. Martin[48], B. Martin dit Latour[17], M. Martinez[14,aa], V. I. Martinez Outschoorn[100], S. Martin-Haugh[141], V. S. Martoiu[27b], A. C. Martyniuk[92], A. Marzin[35], L. Masetti[97], T. Mashimo[160], R. Mashinistov[108], J. Masik[98], A. L. Maslennikov[120a,120b], L. H. Mason[102], L. Massa[71a,71b], P. Massarotti[67a,67b], P. Mastrandrea[5], A. Mastroberardino[40a,40b], T. Masubuchi[160], P. Mättig[179], J. Maurer[27b],

B. Maček[89], S. J. Maxfield[88], D. A. Maximov[120a,120b], R. Mazini[155], I. Maznas[159], S. M. Mazza[143], N. C. Mc Fadden[116], G. Mc Goldrick[164], S. P. Mc Kee[103], A. McCarn[103], T. G. McCarthy[113], L. I. McClymont[92], E. F. McDonald[102], J. A. Mcfayden[35], G. Mchedlidze[51], M. A. McKay[41], K. D. McLean[173], S. J. McMahon[141], P. C. McNamara[102], C. J. McNicol[175], R. A. McPherson[173,ae], J. E. Mdhluli[32c], Z. A. Meadows[100], S. Meehan[145], T. M. Megy[50], S. Mehlhase[112], A. Mehta[88], T. Meideck[56], B. Meirose[42], D. Melini[171,h], B. R. Mellado Garcia[32c], J. D. Mellenthin[51], M. Melo[28a], F. Meloni[44], A. Melzer[24], S. B. Menary[98], E. D. Mendes Gouveia[137a], L. Meng[88], X. T. Meng[103], A. Mengarelli[23a,23b], S. Menke[113], E. Meoni[40a,40b], S. Mergelmeyer[19], C. Merlassino[20], P. Mermod[52], L. Merola[67a,67b], C. Meroni[66a], F. S. Merritt[36], A. Messina[70a,70b], J. Metcalfe[6], A. S. Mete[168], C. Meyer[134], J. Meyer[157], J.-P. Meyer[142], H. Meyer Zu Theenhausen[59a], F. Miano[153], R. P. Middleton[141], L. Mijović[48], G. Mikenberg[177], M. Mikestikova[138], M. Mikuž[89], M. Milesi[102], A. Milic[164], D. A. Millar[90], D. W. Miller[36], A. Milov[177], D. A. Milstead[43a,43b], A. A. Minaenko[121], M. Miñano Moya[171], I. A. Minashvili[156b], A. I. Mincer[122], B. Mindur[81a], M. Mineev[77], Y. Minegishi[160], Y. Ming[178], L. M. Mir[14], A. Mirto[65a,65b], K. P. Mistry[134], T. Mitani[176], J. Mitrevski[112], V. A. Mitsou[171], A. Miucci[20], P. S. Miyagawa[146], A. Mizukami[79], J. U. Mjörnmark[94], T. Mkrtchyan[181], M. Mlynarikova[140], T. Moa[43a,43b], K. Mochizuki[107], P. Mogg[50], S. Mohapatra[38], S. Molander[43a,43b], R. Moles-Valls[24], M. C. Mondragon[104], K. Mönig[44], J. Monk[39], E. Monnier[99], A. Montalbano[149], J. Montejo Berlingen[35], F. Monticelli[86], S. Monzani[66a], N. Morange[129], D. Moreno[22], M. Moreno Llácer[35], P. Morettini[53b], M. Morgenstern[118], S. Morgenstern[46], D. Mori[149], M. Morii[57], M. Morinaga[176], V. Morisbak[131], A. K. Morley[35], G. Mornacchi[35], A. P. Morris[92], J. D. Morris[90], L. Morvaj[152], P. Moschovakos[10], M. Mosidze[156b], H. J. Moss[146], J. Moss[150,o], K. Motohashi[162], R. Mount[150], E. Mountricha[35], E. J. W. Moyse[100], S. Muanza[99], F. Mueller[113], J. Mueller[136], R. S. P. Mueller[112], D. Muenstermann[87], G. A. Mullier[20], F. J. Munoz Sanchez[98], P. Murin[28b], W. J. Murray[141,175], A. Murrone[66a,66b], M. Muškinja[89], C. Mwewa[32a], A. G. Myagkov[121,ao], J. Myers[128], M. Myska[139], B. P. Nachman[18], O. Nackenhorst[45], K. Nagai[132], K. Nagano[79], Y. Nagasaka[60], M. Nagel[50], E. Nagy[99], A. M. Nairz[35], Y. Nakahama[115], K. Nakamura[79], T. Nakamura[160], I. Nakano[124], H. Nanjo[130], F. Napolitano[59a], R. F. Naranjo Garcia[44], R. Narayan[11], D. I. Narrias Villar[59a], I. Naryshkin[135], T. Naumann[44], G. Navarro[22], R. Nayyar[7], H. A. Neal[103,*], P. Y. Nechaeva[108], T. J. Neep[142], A. Negri[68a,68b], M. Negrini[23b], S. Nektarijevic[117], C. Nellist[51], M. E. Nelson[132], S. Nemecek[138], P. Nemethy[122], M. Nessi[35,f], M. S. Neubauer[170], M. Neumann[179], P. R. Newman[21], T. Y. Ng[61c], Y. S. Ng[19], H. D. N. Nguyen[99], T. Nguyen Manh[107], E. Nibigira[37], R. B. Nickerson[132], R. Nicolaidou[142], J. Nielsen[143], N. Nikiforou[11], V. Nikolaenko[121,ao], I. Nikolic-Audit[133], K. Nikolopoulos[21], P. Nilsson[29], Y. Ninomiya[79], A. Nisati[70a], N. Nishu[58c], R. Nisius[113], I. Nitsche[45], T. Nitta[176], T. Nobe[160], Y. Noguchi[83], M. Nomachi[130], I. Nomidis[133], M. A. Nomura[29], T. Nooney[90], M. Nordberg[35], N. Norjoharuddeen[132], T. Novak[89], O. Novgorodova[46], R. Novotny[139], L. Nozka[127], K. Ntekas[168], E. Nurse[92], F. Nuti[102], F. G. Oakham[33,av], H. Oberlack[113], T. Obermann[24], J. Ocariz[133], A. Ochi[80], I. Ochoa[38], J. P. Ochoa-Ricoux[144a], K. O'Connor[26], S. Oda[85], S. Odaka[79], S. Oerdek[51], A. Oh[98], S. H. Oh[47], C. C. Ohm[151], H. Oide[53a,53b], M. L. Ojeda[164], H. Okawa[166], Y. Okazaki[83], Y. Okumura[160], T. Okuyama[79], A. Olariu[27b], L. F. Oleiro Seabra[137a], S. A. Olivares Pino[144a], D. Oliveira Damazio[29], J. L. Oliver[1], M. J. R. Olsson[36], A. Olszewski[82], J. Olszowska[82], D. C. O'Neil[149], A. Onofre[137a,137e], K. Onogi[115], P. U. E. Onyisi[11], H. Oppen[131], M. J. Oreglia[36], G. E. Orellana[86], Y. Oren[158], D. Orestano[72a,72b], E. C. Orgill[98], N. Orlando[61b], A. A. O'Rourke[44], R. S. Orr[164], B. Osculati[53a,53b,*], V. O'Shea[55], R. Ospanov[58a], G. Otero y Garzon[30], H. Otono[85], M. Ouchrif[34d], F. Ould-Saada[131], A. Ouraou[142], Q. Ouyang[15a], M. Owen[55], R. E. Owen[21], V. E. Ozcan[12c], N. Ozturk[8], J. Pacalt[127], H. A. Pacey[31], K. Pachal[149], A. Pacheco Pages[14], L. Pacheco Rodriguez[142], C. Padilla Aranda[14], S. Pagan Griso[18], M. Paganini[180], G. Palacino[63], S. Palazzo[40a,40b], S. Palestini[35], M. Palka[81b], D. Pallin[37], I. Panagoulias[10], C. E. Pandini[35], J. G. Panduro Vazquez[91], P. Pani[35], G. Panizzo[64a,64c], L. Paolozzi[52], T. D. Papadopoulou[10], K. Papageorgiou[9,k], A. Paramonov[6], D. Paredes Hernandez[61b], S. R. Paredes Saenz[132], B. Parida[163], A. J. Parker[87], K. A. Parker[44], M. A. Parker[31], F. Parodi[53a,53b], J. A. Parsons[38], U. Parzefall[50], V. R. Pascuzzi[164], J. M. P. Pasner[143], E. Pasqualucci[70a], S. Passaggio[53b], F. Pastore[91], P. Pasuwan[43a,43b], S. Pataraia[97], J. R. Pater[98], A. Pathak[178,l], T. Pauly[35], B. Pearson[113], M. Pedersen[131], L. Pedraza Diaz[117], R. Pedro[137a,137b], S. V. Peleganchuk[120a,120b], O. Penc[138], C. Peng[15d], H. Peng[58a], B. S. Peralva[78a], M. M. Perego[142], A. P. Pereira Peixoto[137a], D. V. Perepelitsa[29], F. Peri[19], L. Perini[66a,66b], H. Pernegger[35], S. Perrella[67a,67b], V. D. Peshekhonov[77,*], K. Peters[44], R. F. Y. Peters[98], B. A. Petersen[35], T. C. Petersen[39], E. Petit[56], A. Petridis[1], C. Petridou[159], P. Petroff[129], M. Petrov[132], F. Petrucci[72a,72b], M. Pettee[180], N. E. Pettersson[100], A. Peyaud[142], R. Pezoa[144b], T. Pham[102], F. H. Phillips[104], P. W. Phillips[141], M. W. Phipps[170], G. Piacquadio[152], E. Pianori[18], A. Picazio[100], M. A. Pickering[132], R. H. Pickles[98], R. Piegaia[30], J. E. Pilcher[36], A. D. Pilkington[98], M. Pinamonti[71a,71b], J. L. Pinfold[3], M. Pitt[177], M.-A. Pleier[29], V. Pleskot[140], E. Plotnikova[77], D. Pluth[76], P. Podberezko[120a,120b], R. Poettgen[94], R. Poggi[52], L. Poggioli[129], I. Pogrebnyak[104], D. Pohl[24], I. Pokharel[51], G. Polesello[68a], A. Poley[18], A. Policicchio[70a,70b], R. Polifka[35], A. Polini[23b], C. S. Pollard[44], V. Polychronakos[29], D. Ponomarenko[110], L. Pontecorvo[35], G. A. Popeneciu[27d], D. M. Portillo Quintero[133], S. Pospisil[139], K. Potamianos[44], I. N. Potrap[77], C. J. Potter[31], H. Potti[11], T. Poulsen[94],

J. Poveda[35], T. D. Powell[146], M. E. Pozo Astigarraga[35], P. Pralavorio[99], S. Prell[76], D. Price[98], M. Primavera[65a], S. Prince[101], N. Proklova[110], K. Prokofiev[61c], F. Prokoshin[144b], S. Protopopescu[29], J. Proudfoot[6], M. Przybycien[81a], A. Puri[170], P. Puzo[129], J. Qian[103], Y. Qin[98], A. Quadt[51], M. Queitsch-Maitland[44], A. Qureshi[1], P. Rados[102], F. Ragusa[66a,66b], G. Rahal[95], J. A. Raine[52], S. Rajagopalan[29], A. Ramirez Morales[90], T. Rashid[129], S. Raspopov[5], M. G. Ratti[66a,66b], D. M. Rauch[44], F. Rauscher[112], S. Rave[97], B. Ravina[146], I. Ravinovich[177], J. H. Rawling[98], M. Raymond[35], A. L. Read[131], N. P. Readioff[56], M. Reale[65a,65b], D. M. Rebuzzi[68a,68b], A. Redelbach[174], G. Redlinger[29], R. Reece[143], R. G. Reed[32c], K. Reeves[42], L. Rehnisch[19], J. Reichert[134], D. Reikher[158], A. Reiss[97], C. Rembser[35], H. Ren[15d], M. Rescigno[70a], S. Resconi[66a], E. D. Resseguie[134], S. Rettie[172], E. Reynolds[21], O. L. Rezanova[120a,120b], P. Reznicek[140], E. Ricci[73a,73b], R. Richter[113], S. Richter[44], E. Richter-Was[81b], O. Ricken[24], M. Ridel[133], P. Rieck[113], C. J. Riegel[179], O. Rifki[44], M. Rijssenbeek[152], A. Rimoldi[68a,68b], M. Rimoldi[20], L. Rinaldi[23b], G. Ripellino[151], B. Ristić[87], E. Ritsch[35], I. Riu[14], J. C. Rivera Vergara[144a], F. Rizatdinova[126], E. Rizvi[90], C. Rizzi[14], R. T. Roberts[98], S. H. Robertson[101,ae], D. Robinson[31], J. E. M. Robinson[44], A. Robson[55], E. Rocco[97], C. Roda[69a,69b], Y. Rodina[99], S. Rodriguez Bosca[171], A. Rodriguez Perez[14], D. Rodriguez Rodriguez[171], A. M. Rodríguez Vera[165b], S. Roe[35], C. S. Rogan[57], O. Røhne[131], R. Röhrig[113], C. P. A. Roland[63], J. Roloff[57], A. Romaniouk[110], M. Romano[23a,23b], N. Rompotis[88], M. Ronzani[122], L. Roos[133], S. Rosati[70a], K. Rosbach[50], P. Rose[143], N.-A. Rosien[51], E. Rossi[44], E. Rossi[67a,67b], L. P. Rossi[53b], L. Rossini[66a,66b], J. H. N. Rosten[31], R. Rosten[14], M. Rotaru[27b], J. Rothberg[145], D. Rousseau[129], D. Roy[32c], A. Rozanov[99], Y. Rozen[157], X. Ruan[32c], F. Rubbo[150], F. Rühr[50], A. Ruiz-Martinez[171], Z. Rurikova[50], N. A. Rusakovich[77], H. L. Russell[101], J. P. Rutherfoord[7], E. M. Rüttinger[44,m], Y. F. Ryabov[135], M. Rybar[170], G. Rybkin[129], S. Ryu[6], A. Ryzhov[121], G. F. Rzehorz[51], P. Sabatini[51], G. Sabato[118], S. Sacerdoti[129], H. F.-W. Sadrozinski[143], R. Sadykov[77], F. Safai Tehrani[70a], P. Saha[119], M. Sahinsoy[59a], A. Sahu[179], M. Saimpert[44], M. Saito[160], T. Saito[160], H. Sakamoto[160], A. Sakharov[122,an], D. Salamani[52], G. Salamanna[72a,72b], J. E. Salazar Loyola[144b], D. Salek[118], P. H. Sales De Bruin[169], D. Salihagic[113], A. Salnikov[150], J. Salt[171], D. Salvatore[40a,40b], F. Salvatore[153], A. Salvucci[61a,61b,61c], A. Salzburger[35], J. Samarati[35], D. Sammel[50], D. Sampsonidis[159], D. Sampsonidou[159], J. Sánchez[171], A. Sanchez Pineda[64a,64c], H. Sandaker[131], C. O. Sander[44], M. Sandhoff[179], C. Sandoval[22], D. P. C. Sankey[141], M. Sannino[53a,53b], Y. Sano[115], A. Sansoni[49], C. Santoni[37], H. Santos[137a], I. Santoyo Castillo[153], A. Santra[171], A. Sapronov[77], J. G. Saraiva[137a,137d], O. Sasaki[79], K. Sato[166], E. Sauvan[5], P. Savard[164,av], N. Savic[113], R. Sawada[160], C. Sawyer[141], L. Sawyer[93,al], C. Sbarra[23b], A. Sbrizzi[23a], T. Scanlon[92], J. Schaarschmidt[145], P. Schacht[113], B. M. Schachtner[112], D. Schaefer[36], L. Schaefer[134], J. Schaeffer[97], S. Schaepe[35], U. Schäfer[97], A. C. Schaffer[129], D. Schaile[112], R. D. Schamberger[152], N. Scharmberg[98], V. A. Schegelsky[135], D. Scheirich[140], F. Schenck[19], M. Schernau[168], C. Schiavi[53a,53b], S. Schier[143], L. K. Schildgen[24], Z. M. Schillaci[26], E. J. Schioppa[35], M. Schioppa[40a,40b], K. E. Schleicher[50], S. Schlenker[35], K. R. Schmidt-Sommerfeld[113], K. Schmieden[35], C. Schmitt[97], S. Schmitt[44], S. Schmitz[97], J. C. Schmoeckel[44], U. Schnoor[50], L. Schoeffel[142], A. Schoening[59b], E. Schopf[24], M. Schott[97], J. F. P. Schouwenberg[117], J. Schovancova[35], S. Schramm[52], A. Schulte[97], H.-C. Schultz-Coulon[59a], M. Schumacher[50], B. A. Schumm[143], Ph. Schune[142], A. Schwartzman[150], T. A. Schwarz[103], Ph. Schwemling[142], R. Schwienhorst[104], A. Sciandra[24], G. Sciolla[26], M. Scornajenghi[40a,40b], F. Scuri[69a], F. Scutti[102], L. M. Scyboz[113], J. Searcy[103], C. D. Sebastiani[70a,70b], P. Seema[19], S. C. Seidel[116], A. Seiden[143], T. Seiss[36], J. M. Seixas[78b], G. Sekhniaidze[67a], K. Sekhon[103], S. J. Sekula[41], N. Semprini-Cesari[23a,23b], S. Sen[47], S. Senkin[37], C. Serfon[131], L. Serin[129], L. Serkin[64a,64b], M. Sessa[58a], H. Severini[125], F. Sforza[167], A. Sfyrla[52], E. Shabalina[51], J. D. Shahinian[143], N. W. Shaikh[43a,43b], L. Y. Shan[15a], R. Shang[170], J. T. Shank[25], M. Shapiro[18], A. S. Sharma[1], A. Sharma[132], P. B. Shatalov[109], K. Shaw[153], S. M. Shaw[98], A. Shcherbakova[135], Y. Shen[125], N. Sherafati[33], A. D. Sherman[25], P. Sherwood[92], L. Shi[155,ar], S. Shimizu[79], C. O. Shimmin[180], M. Shimojima[114], I. P. J. Shipsey[132], S. Shirabe[85], M. Shiyakova[77], J. Shlomi[177], A. Shmeleva[108], D. Shoaleh Saadi[107], M. J. Shochet[36], S. Shojaii[102], D. R. Shope[125], S. Shrestha[123], E. Shulga[110], P. Sicho[138], A. M. Sickles[170], P. E. Sidebo[151], E. Sideras Haddad[32c], O. Sidiropoulou[35], A. Sidoti[23a,23b], F. Siegert[46], Dj. Sijacki[16], J. Silva[137a], M. Silva Jr.[178], M. V. Silva Oliveira[78a], S. B. Silverstein[43a], L. Simic[77], S. Simion[129], E. Simioni[97], M. Simon[97], R. Simoniello[97], P. Sinervo[164], N. B. Sinev[128], M. Sioli[23a,23b], G. Siragusa[174], I. Siral[103], S. Yu. Sivoklokov[111], J. Sjölin[43a,43b], P. Skubic[125], M. Slater[21], T. Slavicek[139], M. Slawinska[82], K. Sliwa[167], R. Slovak[140], V. Smakhtin[177], B. H. Smart[5], J. Smiesko[28a], N. Smirnov[110], S. Yu. Smirnov[110], Y. Smirnov[110], L. N. Smirnova[111], O. Smirnova[94], J. W. Smith[51], M. N. K. Smith[38], M. Smizanska[87], K. Smolek[139], A. Smykiewicz[82], A. A. Snesarev[108], I. M. Snyder[128], S. Snyder[29], R. Sobie[173,ae], A. M. Soffa[168], A. Soffer[158], A. Søgaard[48], D. A. Soh[155], G. Sokhrannyi[89], C. A. Solans Sanchez[35], M. Solar[139], E. Yu. Soldatov[110], U. Soldevila[171], A. A. Solodkov[121], A. Soloshenko[77], O. V. Solovyanov[121], V. Solovyev[135], P. Sommer[146], H. Son[167], W. Song[141], W. Y. Song[165b], A. Sopczak[139], F. Sopkova[28b], C. L. Sotiropoulou[69a,69b], S. Sottocornola[68a,68b], R. Soualah[64a,64c,j], A. M. Soukharev[120a,120b], D. South[44], B. C. Sowden[91], S. Spagnolo[65a,65b], M. Spalla[113], M. Spangenberg[175], F. Spanò[91], D. Sperlich[19], F. Spettel[113], T. M. Spieker[59a], R. Spighi[23b], G. Spigo[35], L. A. Spiller[102], D. P. Spiteri[55],

M. Spousta[140], A. Stabile[66a,66b], R. Stamen[59a], S. Stamm[19], E. Stanecka[82], R. W. Stanek[6], C. Stanescu[72a], B. Stanislaus[132], M. M. Stanitzki[44], B. Stapf[118], S. Stapnes[131], E. A. Starchenko[121], G. H. Stark[36], J. Stark[56], S. H Stark[39], P. Staroba[138], P. Starovoitov[59a], S. Stärz[35], R. Staszewski[82], M. Stegler[44], P. Steinberg[29], B. Stelzer[149], H. J. Stelzer[35], O. Stelzer-Chilton[165a], H. Stenzel[54], T. J. Stevenson[90], G. A. Stewart[35], M. C. Stockton[128], G. Stoicea[27b], P. Stolte[51], S. Stonjek[113], A. Straessner[46], J. Strandberg[151], S. Strandberg[43a,43b], M. Strauss[125], P. Strizenec[28b], R. Ströhmer[174], D. M. Strom[128], R. Stroynowski[41], A. Strubig[48], S. A. Stucci[29], B. Stugu[17], J. Stupak[125], N. A. Styles[44], D. Su[150], J. Su[136], S. Suchek[59a], Y. Sugaya[130], M. Suk[139], V. V. Sulin[108], D. M. S. Sultan[52], S. Sultansoy[4c], T. Sumida[83], S. Sun[103], X. Sun[3], K. Suruliz[153], C. J. E. Suster[154], M. R. Sutton[153], S. Suzuki[79], M. Svatos[138], M. Swiatlowski[36], S. P. Swift[2], A. Sydorenko[97], I. Sykora[28a], T. Sykora[140], D. Ta[97], K. Tackmann[44,ab], J. Taenzer[158], A. Taffard[168], R. Tafirout[165a], E. Tahirovic[90], N. Taiblum[158], H. Takai[29], R. Takashima[84], E. H. Takasugi[113], K. Takeda[80], T. Takeshita[147], Y. Takubo[79], M. Talby[99], A. A. Talyshev[120a,120b], J. Tanaka[160], M. Tanaka[162], R. Tanaka[129], B. B. Tannenwald[123], S. Tapia Araya[144b], S. Tapprogge[97], A. Tarek Abouelfadl Mohamed[133], S. Tarem[157], G. Tarna[27b,e], G. F. Tartarelli[66a], P. Tas[140], M. Tasevsky[138], T. Tashiro[83], E. Tassi[40a,40b], A. Tavares Delgado[137a,137b], Y. Tayalati[34e], A. C. Taylor[116], A. J. Taylor[48], G. N. Taylor[102], P. T. E. Taylor[102], W. Taylor[165b], A. S. Tee[87], P. Teixeira-Dias[91], H. Ten Kate[35], P. K. Teng[155], J. J. Teoh[118], S. Terada[79], K. Terashi[160], J. Terron[96], S. Terzo[14], M. Testa[49], R. J. Teuscher[164,ae], S. J. Thais[180], T. Theveneaux-Pelzer[44], F. Thiele[39], D. W. Thomas[91], J. P. Thomas[21], A. S. Thompson[55], P. D. Thompson[21], L. A. Thomsen[180], E. Thomson[134], Y. Tian[38], R. E. Ticse Torres[51], V. O. Tikhomirov[108,ap], Yu. A. Tikhonov[120a,120b], S. Timoshenko[110], P. Tipton[180], S. Tisserant[99], K. Todome[162], S. Todorova-Nova[5], S. Todt[46], J. Tojo[85], S. Tokár[28a], K. Tokushuku[79], E. Tolley[123], K. G. Tomiwa[32c], M. Tomoto[115], L. Tompkins[150,r], K. Toms[116], B. Tong[57], P. Tornambe[50], E. Torrence[128], H. Torres[46], E. Torró Pastor[145], C. Tosciri[132], J. Toth[99,ad], F. Touchard[99], D. R. Tovey[146], C. J. Treado[122], T. Trefzger[174], F. Tresoldi[153], A. Tricoli[29], I. M. Trigger[165a], S. Trincaz-Duvoid[133], M. F. Tripiana[14], W. Trischuk[164], B. Trocmé[56], A. Trofymov[129], C. Troncon[66a], M. Trovatelli[173], F. Trovato[153], L. Truong[32b], M. Trzebinski[82], A. Trzupek[82], F. Tsai[44], J. C.-L. Tseng[132], P. V. Tsiareshka[105], A. Tsirigotis[159], N. Tsirintanis[9], V. Tsiskaridze[152], E. G. Tskhadadze[156a], I. I. Tsukerman[109], V. Tsulaia[18], S. Tsuno[79], D. Tsybychev[152,163], Y. Tu[61b], A. Tudorache[27b], V. Tudorache[27b], T. T. Tulbure[27a], A. N. Tuna[57], S. Turchikhin[77], D. Turgeman[177], I. Turk Cakir[4b,v], R. Turra[66a], P. M. Tuts[38], E. Tzovara[97], G. Ucchielli[23a,23b], I. Ueda[79], M. Ughetto[43a,43b], F. Ukegawa[166], G. Unal[35], A. Undrus[29], G. Unel[168], F. C. Ungaro[102], Y. Unno[79], K. Uno[160], J. Urban[28b], P. Urquijo[102], P. Urrejola[97], G. Usai[8], J. Usui[79], L. Vacavant[99], V. Vacek[139], B. Vachon[101], K. O. H. Vadla[131], A. Vaidya[92], C. Valderanis[112], E. Valdes Santurio[43a,43b], M. Valente[52], S. Valentinetti[23a,23b], A. Valero[171], L. Valéry[44], R. A. Vallance[21], A. Vallier[5], J. A. Valls Ferrer[171], T. R. Van Daalen[14], H. Van der Graaf[118], P. Van Gemmeren[6], J. Van Nieuwkoop[149], I. Van Vulpen[118], M. Vanadia[71a,71b], W. Vandelli[35], A. Vaniachine[163], P. Vankov[118], R. Vari[70a], E. W. Varnes[7], C. Varni[53a,53b], T. Varol[41], D. Varouchas[129], K. E. Varvell[154], G. A. Vasquez[144b], J. G. Vasquez[180], F. Vazeille[37], D. Vazquez Furelos[14], T. Vazquez Schroeder[101], J. Veatch[51], V. Vecchio[72a,72b], L. M. Veloce[164], F. Veloso[137a,137c], S. Veneziano[70a], A. Ventura[65a,65b], M. Venturi[173], N. Venturi[35], V. Vercesi[68a], M. Verducci[72a,72b], C. M. Vergel Infante[76], C. Vergis[24], W. Verkerke[118], A. T. Vermeulen[118], J. C. Vermeulen[118], M. C. Vetterli[149,av], N. Viaux Maira[144b], M. Vicente Barreto Pinto[52], I. Vichou[170,*], T. Vickey[146], O. E. Vickey Boeriu[146], G. H. A. Viehhauser[132], S. Viel[18], L. Vigani[132], M. Villa[23a,23b], M. Villaplana Perez[66a,66b], E. Vilucchi[49], M. G. Vincter[33], V. B. Vinogradov[77], A. Vishwakarma[44], C. Vittori[23a,23b], I. Vivarelli[153], S. Vlachos[10], M. Vogel[179], P. Vokac[139], G. Volpi[14], S. E. Von Buddenbrock[32c], E. von Toerne[24], V. Vorobel[140], K. Vorobev[110], M. Vos[171], J. H. Vossebeld[88], N. Vranjes[16], M. Vranjes Milosavljevic[16], V. Vrba[139], M. Vreeswijk[118], T. Šfiligoj[89], R. Vuillermet[35], I. Vukotic[36], T. Ženiš[28a], L. Živković[16], P. Wagner[24], W. Wagner[179], J. Wagner-Kuhr[112], H. Wahlberg[86], S. Wahrmund[46], K. Wakamiya[80], V. M. Walbrecht[113], J. Walder[87], R. Walker[112], S. D. Walker[91], W. Walkowiak[148], V. Wallangen[43a,43b], A. M. Wang[57], C. Wang[58b,e], F. Wang[178], H. Wang[18], H. Wang[3], J. Wang[154], J. Wang[59b], P. Wang[41], Q. Wang[125], R.-J. Wang[133], R. Wang[58a], R. Wang[6], S. M. Wang[155], T. Wang[58a], W. Wang[15c,af], W. X. Wang[58a,af], Y. Wang[58a,am], Z. Wang[58c], C. Wanotayaroj[44], A. Warburton[101], C. P. Ward[31], D. R. Wardrope[92], A. Washbrook[48], P. M. Watkins[21], A. T. Watson[21], M. F. Watson[21], G. Watts[145], S. Watts[98], B. M. Waugh[92], A. F. Webb[11], S. Webb[97], C. Weber[180], M. S. Weber[20], S. A. Weber[33], S. M. Weber[59a], A. R. Weidberg[132], B. Weinert[63], J. Weingarten[45], M. Weirich[97], C. Weiser[50], P. S. Wells[35], T. Wenaus[29], T. Wengler[35], S. Wenig[35], N. Wermes[24], M. D. Werner[76], P. Werner[35], M. Wessels[59a], T. D. Weston[20], K. Whalen[128], N. L. Whallon[145], A. M. Wharton[87], A. S. White[103], A. White[8], M. J. White[1], R. White[144b], D. Whiteson[168], B. W. Whitmore[87], F. J. Wickens[141], W. Wiedenmann[178], M. Wielers[141], C. Wiglesworth[39], L. A. M. Wiik-Fuchs[50], A. Wildauer[113], F. Wilk[98], H. G. Wilkens[35], L. J. Wilkins[91], H. H. Williams[134], S. Williams[31], C. Willis[104], S. Willocq[100], J. A. Wilson[21], I. Wingerter-Seez[5], E. Winkels[153], F. Winklmeier[128], O. J. Winston[153], B. T. Winter[24], M. Wittgen[150], M. Wobisch[93], A. Wolf[97], T. M. H. Wolf[118], R. Wolff[99], M. W. Wolter[82], H. Wolters[137a,137c], V. W. S. Wong[172], N. L. Woods[143], S. D. Worm[21], B. K. Wosiek[82], K. W. Woźniak[82], K. Wraight[55], M. Wu[36], S. L. Wu[178],

X. Wu[52], Y. Wu[58a], T. R. Wyatt[98], B. M. Wynne[48], S. Xella[39], Z. Xi[103], L. Xia[175], D. Xu[15a], H. Xu[58a,e], L. Xu[29], T. Xu[142], W. Xu[103], B. Yabsley[154], S. Yacoob[32a], K. Yajima[130], D. P. Yallup[92], D. Yamaguchi[162], Y. Yamaguchi[162], A. Yamamoto[79], T. Yamanaka[160], F. Yamane[80], M. Yamatani[160], T. Yamazaki[160], Y. Yamazaki[80], Z. Yan[25], H. J. Yang[58c,58d], H. T. Yang[18], S. Yang[75], Y. Yang[160], Z. Yang[17], W-M. Yao[18], Y. C. Yap[44], Y. Yasu[79], E. Yatsenko[58c,58d], J. Ye[41], S. Ye[29], I. Yeletskikh[77], E. Yigitbasi[25], E. Yildirim[97], K. Yorita[176], K. Yoshihara[134], C. J. S. Young[35], C. Young[150], J. Yu[8], J. Yu[76], X. Yue[59a], S. P. Y. Yuen[24], B. Zabinski[82], G. Zacharis[10], E. Zaffaroni[52], R. Zaidan[14], A. M. Zaitsev[121,ao], T. Zakareishvili[156b], N. Zakharchuk[33], J. Zalieckas[17], S. Zambito[57], D. Zanzi[35], D. R. Zaripovas[55], S. V. Zeißner[45], C. Zeitnitz[179], G. Zemaityte[132], J. C. Zeng[170], Q. Zeng[150], O. Zenin[121], D. Zerwas[129], M. Zgubič[132], D. F. Zhang[58b], D. Zhang[103], F. Zhang[178], G. Zhang[58a], H. Zhang[15c], J. Zhang[6], L. Zhang[15c], L. Zhang[58a], M. Zhang[170], P. Zhang[15c], R. Zhang[58a], R. Zhang[24], X. Zhang[58b], Y. Zhang[15d], Z. Zhang[129], P. Zhao[47], X. Zhao[41], Y. Zhao[58b,129,ak], Z. Zhao[58a], A. Zhemchugov[77], B. Zhou[103], C. Zhou[178], L. Zhou[41], M. S. Zhou[15d], M. Zhou[152], N. Zhou[58c], Y. Zhou[7], C. G. Zhu[58b], H. L. Zhu[58a], H. Zhu[15a], J. Zhu[103], Y. Zhu[58a], X. Zhuang[15a], K. Zhukov[108], V. Zhulanov[120a,120b], A. Zibell[174], D. Zieminska[63], N. I. Zimine[77], S. Zimmermann[50], Z. Zinonos[113], M. Zinser[97], M. Ziolkowski[148], G. Zobernig[178], A. Zoccoli[23a,23b], K. Zoch[51], T. G. Zorbas[146], R. Zou[36], M. Zur Nedden[19], L. Zwalinski[35]

[1] Department of Physics, University of Adelaide, Adelaide, Australia

[2] Physics Department, SUNY Albany, Albany, NY, USA

[3] Department of Physics, University of Alberta, Edmonton, AB, Canada

[4] (a)Department of Physics, Ankara University, Ankara, Turkey; (b)Istanbul Aydin University, Istanbul, Turkey; (c)Division of Physics, TOBB University of Economics and Technology, Ankara, Turkey

[5] LAPP, Université Grenoble Alpes, Université Savoie Mont Blanc, CNRS/IN2P3, Annecy, France

[6] High Energy Physics Division, Argonne National Laboratory, Argonne, IL, USA

[7] Department of Physics, University of Arizona, Tucson, AZ, USA

[8] Department of Physics, University of Texas at Arlington, Arlington, TX, USA

[9] Physics Department, National and Kapodistrian University of Athens, Athens, Greece

[10] Physics Department, National Technical University of Athens, Zografou, Greece

[11] Department of Physics, University of Texas at Austin, Austin, TX, USA

[12] (a)Faculty of Engineering and Natural Sciences, Bahcesehir University, Istanbul, Turkey; (b)Faculty of Engineering and Natural Sciences, Istanbul Bilgi University, Istanbul, Turkey; (c)Department of Physics, Bogazici University, Istanbul, Turkey; (d)Department of Physics Engineering, Gaziantep University, Gaziantep, Turkey

[13] Institute of Physics, Azerbaijan Academy of Sciences, Baku, Azerbaijan

[14] Institut de Física d'Altes Energies (IFAE), Barcelona Institute of Science and Technology, Barcelona, Spain

[15] (a)Institute of High Energy Physics, Chinese Academy of Sciences, Beijing, China; (b)Physics Department, Tsinghua University, Beijing, China; (c)Department of Physics, Nanjing University, Nanjing, China; (d)University of Chinese Academy of Science (UCAS), Beijing, China

[16] Institute of Physics, University of Belgrade, Belgrade, Serbia

[17] Department for Physics and Technology, University of Bergen, Bergen, Norway

[18] Physics Division, Lawrence Berkeley National Laboratory and University of California, Berkeley, CA, USA

[19] Institut für Physik, Humboldt Universität zu Berlin, Berlin, Germany

[20] Albert Einstein Center for Fundamental Physics and Laboratory for High Energy Physics, University of Bern, Bern, Switzerland

[21] School of Physics and Astronomy, University of Birmingham, Birmingham, UK

[22] Centro de Investigaciónes, Universidad Antonio Nariño, Bogotá, Colombia

[23] (a)Dipartimento di Fisica e Astronomia, Università di Bologna, Bologna, Italy; (b)INFN Sezione di Bologna, Bologna, Italy

[24] Physikalisches Institut, Universität Bonn, Bonn, Germany

[25] Department of Physics, Boston University, Boston, MA, USA

[26] Department of Physics, Brandeis University, Waltham, MA, USA

[27] (a)Transilvania University of Brasov, Brasov, Romania; (b)Horia Hulubei National Institute of Physics and Nuclear Engineering, Bucharest, Romania; (c)Department of Physics, Alexandru Ioan Cuza University of Iasi, Iasi, Romania; (d)Physics Department, National Institute for Research and Development of Isotopic and Molecular Technologies, Cluj-Napoca, Romania; (e)University Politehnica Bucharest, Bucharest, Romania; (f)West University in Timisoara, Timisoara, Romania

28 (a)Faculty of Mathematics, Physics and Informatics, Comenius University, Bratislava, Slovakia; (b)Department of Subnuclear Physics, Institute of Experimental Physics of the Slovak Academy of Sciences, Kosice, Slovak Republic

29 Physics Department, Brookhaven National Laboratory, Upton, NY, USA

30 Departamento de Física, Universidad de Buenos Aires, Buenos Aires, Argentina

31 Cavendish Laboratory, University of Cambridge, Cambridge, UK

32 (a)Department of Physics, University of Cape Town, Cape Town, South Africa; (b)Department of Mechanical Engineering Science, University of Johannesburg, Johannesburg, South Africa; (c)School of Physics, University of the Witwatersrand, Johannesburg, South Africa

33 Department of Physics, Carleton University, Ottawa, ON, Canada

34 (a)Faculté des Sciences Ain Chock, Réseau Universitaire de Physique des Hautes Energies-Université Hassan II, Casablanca, Morocco; (b)Centre National de l'Energie des Sciences Techniques Nucleaires (CNESTEN), Rabat, Morocco; (c)Faculté des Sciences Semlalia, Université Cadi Ayyad, LPHEA-Marrakech, Marrakech, Morocco; (d)Faculté des Sciences, Université Mohamed Premier and LPTPM, Oujda, Morocco; (e)Faculté des sciences, Université Mohammed V, Rabat, Morocco

35 CERN, Geneva, Switzerland

36 Enrico Fermi Institute, University of Chicago, Chicago, IL, USA

37 LPC, Université Clermont Auvergne, CNRS/IN2P3, Clermont-Ferrand, France

38 Nevis Laboratory, Columbia University, Irvington, NY, USA

39 Niels Bohr Institute, University of Copenhagen, Copenhagen, Denmark

40 (a)Dipartimento di Fisica, Università della Calabria, Rende, Italy; (b)INFN Gruppo Collegato di Cosenza, Laboratori Nazionali di Frascati, Frascati, Italy

41 Physics Department, Southern Methodist University, Dallas, TX, USA

42 Physics Department, University of Texas at Dallas, Richardson, TX, USA

43 (a)Department of Physics, Stockholm University, Stockholm, Sweden; (b)Oskar Klein Centre, Stockholm, Sweden

44 Deutsches Elektronen-Synchrotron DESY, Hamburg and Zeuthen, Germany

45 Lehrstuhl für Experimentelle Physik IV, Technische Universität Dortmund, Dortmund, Germany

46 Institut für Kern- und Teilchenphysik, Technische Universität Dresden, Dresden, Germany

47 Department of Physics, Duke University, Durham, NC, USA

48 SUPA-School of Physics and Astronomy, University of Edinburgh, Edinburgh, UK

49 INFN e Laboratori Nazionali di Frascati, Frascati, Italy

50 Physikalisches Institut, Albert-Ludwigs-Universität Freiburg, Freiburg, Germany

51 II. Physikalisches Institut, Georg-August-Universität Göttingen, Göttingen, Germany

52 Département de Physique Nucléaire et Corpusculaire, Université de Genève, Geneva, Switzerland

53 (a)Dipartimento di Fisica, Università di Genova, Genoa, Italy; (b)INFN Sezione di Genova, Genoa, Italy

54 II. Physikalisches Institut, Justus-Liebig-Universität Giessen, Giessen, Germany

55 SUPA-School of Physics and Astronomy, University of Glasgow, Glasgow, UK

56 LPSC, Université Grenoble Alpes, CNRS/IN2P3, Grenoble INP, Grenoble, France

57 Laboratory for Particle Physics and Cosmology, Harvard University, Cambridge, MA, USA

58 (a)Department of Modern Physics and State Key Laboratory of Particle Detection and Electronics, University of Science and Technology of China, Hefei, China; (b)Institute of Frontier and Interdisciplinary Science and Key Laboratory of Particle Physics and Particle Irradiation (MOE), Shandong University, Qingdao, China; (c)School of Physics and Astronomy, Shanghai Jiao Tong University, KLPPAC-MoE, SKLPPC, Shanghai, China; (d)Tsung-Dao Lee Institute, Shanghai, China

59 (a)Kirchhoff-Institut für Physik, Ruprecht-Karls-Universität Heidelberg, Heidelberg, Germany; (b)Physikalisches Institut, Ruprecht-Karls-Universität Heidelberg, Heidelberg, Germany

60 Faculty of Applied Information Science, Hiroshima Institute of Technology, Hiroshima, Japan

61 (a)Department of Physics, Chinese University of Hong Kong, Shatin, NT, Hong Kong; (b)Department of Physics, University of Hong Kong, Hong Kong, China; (c)Department of Physics and Institute for Advanced Study, Hong Kong University of Science and Technology, Clear Water Bay, Kowloon, Hong Kong, China

62 Department of Physics, National Tsing Hua University, Hsinchu, Taiwan

63 Department of Physics, Indiana University, Bloomington, IN, USA

64 (a)INFN Gruppo Collegato di Udine, Sezione di Trieste, Udine, Italy; (b)ICTP, Trieste, Italy; (c)Dipartimento di Chimica, Fisica e Ambiente, Università di Udine, Udine, Italy

65 (a)INFN Sezione di Lecce, Lecce, Italy; (b)Dipartimento di Matematica e Fisica, Università del Salento, Lecce, Italy

66 (a)INFN Sezione di Milano, Milan, Italy; (b)Dipartimento di Fisica, Università di Milano, Milan, Italy

67 (a)INFN Sezione di Napoli, Naples, Italy; (b)Dipartimento di Fisica, Università di Napoli, Naples, Italy

68 (a)INFN Sezione di Pavia, Pavia, Italy; (b)Dipartimento di Fisica, Università di Pavia, Pavia, Italy

69 (a)INFN Sezione di Pisa, Pisa, Italy; (b)Dipartimento di Fisica E. Fermi, Università di Pisa, Pisa, Italy

70 (a)INFN Sezione di Roma, Rome, Italy; (b)Dipartimento di Fisica, Sapienza Università di Roma, Rome, Italy

71 (a)INFN Sezione di Roma Tor Vergata, Rome, Italy; (b)Dipartimento di Fisica, Università di Roma Tor Vergata, Rome, Italy

72 (a)INFN Sezione di Roma Tre, Rome, Italy; (b)Dipartimento di Matematica e Fisica, Università Roma Tre, Rome, Italy

73 (a)INFN-TIFPA, Povo, Italy; (b)Università degli Studi di Trento, Trento, Italy

74 Institut für Astro- und Teilchenphysik, Leopold-Franzens-Universität, Innsbruck, Austria

75 University of Iowa, Iowa City, IA, USA

76 Department of Physics and Astronomy, Iowa State University, Ames, IA, USA

77 Joint Institute for Nuclear Research, Dubna, Russia

78 (a)Departamento de Engenharia Elétrica, Universidade Federal de Juiz de Fora (UFJF), Juiz de Fora, Brazil; (b)Universidade Federal do Rio De Janeiro COPPE/EE/IF, Rio de Janeiro, Brazil; (c)Universidade Federal de São João del Rei (UFSJ), São João del Rei, Brazil; (d)Instituto de Física, Universidade de São Paulo, São Paulo, Brazil

79 KEK, High Energy Accelerator Research Organization, Tsukuba, Japan

80 Graduate School of Science, Kobe University, Kobe, Japan

81 (a)Faculty of Physics and Applied Computer Science, AGH University of Science and Technology, Kraków, Poland; (b)Marian Smoluchowski Institute of Physics, Jagiellonian University, Kraków, Poland

82 Institute of Nuclear Physics Polish Academy of Sciences, Kraków, Poland

83 Faculty of Science, Kyoto University, Kyoto, Japan

84 Kyoto University of Education, Kyoto, Japan

85 Research Center for Advanced Particle Physics and Department of Physics, Kyushu University, Fukuoka, Japan

86 Instituto de Física La Plata, Universidad Nacional de La Plata and CONICET, La Plata, Argentina

87 Physics Department, Lancaster University, Lancaster, UK

88 Oliver Lodge Laboratory, University of Liverpool, Liverpool, UK

89 Department of Experimental Particle Physics, Jožef Stefan Institute and Department of Physics, University of Ljubljana, Ljubljana, Slovenia

90 School of Physics and Astronomy, Queen Mary University of London, London, UK

91 Department of Physics, Royal Holloway University of London, Egham, UK

92 Department of Physics and Astronomy, University College London, London, UK

93 Louisiana Tech University, Ruston, LA, USA

94 Fysiska institutionen, Lunds universitet, Lund, Sweden

95 Centre de Calcul de l'Institut National de Physique Nucléaire et de Physique des Particules (IN2P3), Villeurbanne, France

96 Departamento de Física Teorica C-15 and CIAFF, Universidad Autónoma de Madrid, Madrid, Spain

97 Institut für Physik, Universität Mainz, Mainz, Germany

98 School of Physics and Astronomy, University of Manchester, Manchester, UK

99 CPPM, Aix-Marseille Université, CNRS/IN2P3, Marseille, France

100 Department of Physics, University of Massachusetts, Amherst, MA, USA

101 Department of Physics, McGill University, Montreal, QC, Canada

102 School of Physics, University of Melbourne, Parkville, VIC, Australia

103 Department of Physics, University of Michigan, Ann Arbor, MI, USA

104 Department of Physics and Astronomy, Michigan State University, East Lansing, MI, USA

105 B.I. Stepanov Institute of Physics, National Academy of Sciences of Belarus, Minsk, Belarus

106 Research Institute for Nuclear Problems of Byelorussian State University, Minsk, Belarus

107 Group of Particle Physics, University of Montreal, Montreal, QC, Canada

108 P.N. Lebedev Physical Institute of the Russian Academy of Sciences, Moscow, Russia

109 Institute for Theoretical and Experimental Physics (ITEP), Moscow, Russia

110 National Research Nuclear University MEPhI, Moscow, Russia

111 D.V. Skobeltsyn Institute of Nuclear Physics, M.V. Lomonosov Moscow State University, Moscow, Russia

[112] Fakultät für Physik, Ludwig-Maximilians-Universität München, Munich, Germany

[113] Max-Planck-Institut für Physik (Werner-Heisenberg-Institut), Munich, Germany

[114] Nagasaki Institute of Applied Science, Nagasaki, Japan

[115] Graduate School of Science and Kobayashi-Maskawa Institute, Nagoya University, Nagoya, Japan

[116] Department of Physics and Astronomy, University of New Mexico, Albuquerque, NM, USA

[117] Institute for Mathematics, Astrophysics and Particle Physics, Radboud University Nijmegen/Nikhef, Nijmegen, The Netherlands

[118] Nikhef National Institute for Subatomic Physics, University of Amsterdam, Amsterdam, The Netherlands

[119] Department of Physics, Northern Illinois University, De Kalb, IL, USA

[120] [a]Budker Institute of Nuclear Physics and NSU, SB RAS, Novosibirsk, Russia; [b]Novosibirsk State University, Novosibirsk, Russia

[121] Institute for High Energy Physics of the National Research Centre Kurchatov Institute, Protvino, Russia

[122] Department of Physics, New York University, New York, NY, USA

[123] Ohio State University, Columbus, OH, USA

[124] Faculty of Science, Okayama University, Okayama, Japan

[125] Homer L. Dodge Department of Physics and Astronomy, University of Oklahoma, Norman, OK, USA

[126] Department of Physics, Oklahoma State University, Stillwater, OK, USA

[127] Palacký University, RCPTM, Joint Laboratory of Optics, Olomouc, Czech Republic

[128] Center for High Energy Physics, University of Oregon, Eugene, OR, USA

[129] LAL, Université Paris-Sud, CNRS/IN2P3, Université Paris-Saclay, Orsay, France

[130] Graduate School of Science, Osaka University, Osaka, Japan

[131] Department of Physics, University of Oslo, Oslo, Norway

[132] Department of Physics, Oxford University, Oxford, UK

[133] LPNHE, Sorbonne Université, Paris Diderot Sorbonne Paris Cité, CNRS/IN2P3, Paris, France

[134] Department of Physics, University of Pennsylvania, Philadelphia, PA, USA

[135] Konstantinov Nuclear Physics Institute of National Research Centre "Kurchatov Institute", PNPI, St. Petersburg, Russia

[136] Department of Physics and Astronomy, University of Pittsburgh, Pittsburgh, PA, USA

[137] [a]Laboratório de Instrumentação e Física Experimental de Partículas-LIP, Lisbon, Portugal; [b]Departamento de Física, Faculdade de Ciências, Universidade de Lisboa, Lisbon, Portugal; [c]Departamento de Física, Universidade de Coimbra, Coimbra, Portugal; [d]Centro de Física Nuclear da Universidade de Lisboa, Lisbon, Portugal; [e]Departamento de Física, Universidade do Minho, Braga, Portugal; [f]Departamento de Física Teorica y del Cosmos, Universidad de Granada, Granada, Spain; [g]Dep Física and CEFITEC of Faculdade de Ciências e Tecnologia, Universidade Nova de Lisboa, Caparica, Portugal

[138] Institute of Physics, Academy of Sciences of the Czech Republic, Prague, Czech Republic

[139] Czech Technical University in Prague, Prague, Czech Republic

[140] Faculty of Mathematics and Physics, Charles University, Prague, Czech Republic

[141] Particle Physics Department, Rutherford Appleton Laboratory, Didcot, UK

[142] IRFU, CEA, Université Paris-Saclay, Gif-sur-Yvette, France

[143] Santa Cruz Institute for Particle Physics, University of California Santa Cruz, Santa Cruz, CA, USA

[144] [a]Departamento de Física, Pontificia Universidad Católica de Chile, Santiago, Chile; [b]Departamento de Física, Universidad Técnica Federico Santa María, Valparaiso, Chile

[145] Department of Physics, University of Washington, Seattle, WA, USA

[146] Department of Physics and Astronomy, University of Sheffield, Sheffield, UK

[147] Department of Physics, Shinshu University, Nagano, Japan

[148] Department Physik, Universität Siegen, Siegen, Germany

[149] Department of Physics, Simon Fraser University, Burnaby, BC, Canada

[150] SLAC National Accelerator Laboratory, Stanford, CA, USA

[151] Physics Department, Royal Institute of Technology, Stockholm, Sweden

[152] Departments of Physics and Astronomy, Stony Brook University, Stony Brook, NY, USA

[153] Department of Physics and Astronomy, University of Sussex, Brighton, UK

[154] School of Physics, University of Sydney, Sydney, Australia

[155] Institute of Physics, Academia Sinica, Taipei, Taiwan

156 (a)E. Andronikashvili Institute of Physics, Iv. Javakhishvili Tbilisi State University, Tbilisi, Georgia; (b)High Energy Physics Institute, Tbilisi State University, Tbilisi, Georgia

157 Department of Physics, Technion, Israel Institute of Technology, Haifa, Israel

158 Raymond and Beverly Sackler School of Physics and Astronomy, Tel Aviv University, Tel Aviv, Israel

159 Department of Physics, Aristotle University of Thessaloniki, Thessaloníki, Greece

160 International Center for Elementary Particle Physics and Department of Physics, University of Tokyo, Tokyo, Japan

161 Graduate School of Science and Technology, Tokyo Metropolitan University, Tokyo, Japan

162 Department of Physics, Tokyo Institute of Technology, Tokyo, Japan

163 Tomsk State University, Tomsk, Russia

164 Department of Physics, University of Toronto, Toronto, ON, Canada

165 (a)TRIUMF, Vancouver, BC, Canada; (b)Department of Physics and Astronomy, York University, Toronto, ON, Canada

166 Division of Physics and Tomonaga Center for the History of the Universe, Faculty of Pure and Applied Sciences, University of Tsukuba, Tsukuba, Japan

167 Department of Physics and Astronomy, Tufts University, Medford, MA, USA

168 Department of Physics and Astronomy, University of California Irvine, Irvine, CA, USA

169 Department of Physics and Astronomy, University of Uppsala, Uppsala, Sweden

170 Department of Physics, University of Illinois, Urbana, IL, USA

171 Instituto de Física Corpuscular (IFIC), Centro Mixto Universidad de Valencia, CSIC, Valencia, Spain

172 Department of Physics, University of British Columbia, Vancouver, BC, Canada

173 Department of Physics and Astronomy, University of Victoria, Victoria, BC, Canada

174 Fakultät für Physik und Astronomie, Julius-Maximilians-Universität Würzburg, Würzburg, Germany

175 Department of Physics, University of Warwick, Coventry, UK

176 Waseda University, Tokyo, Japan

177 Department of Particle Physics, Weizmann Institute of Science, Rehovot, Israel

178 Department of Physics, University of Wisconsin, Madison, WI, USA

179 Fakultät für Mathematik und Naturwissenschaften, Fachgruppe Physik, Bergische Universität Wuppertal, Wuppertal, Germany

180 Department of Physics, Yale University, New Haven, CT, USA

181 Yerevan Physics Institute, Yerevan, Armenia

a Also at Borough of Manhattan Community College, City University of New York, NY, USA

b Also at California State University, East Bay, USA

c Also at Centre for High Performance Computing, CSIR Campus, Rosebank, Cape Town, South Africa

d Also at CERN, Geneva, Switzerland

e Also at CPPM, Aix-Marseille Université, CNRS/IN2P3, Marseille, France

f Also at Département de Physique Nucléaire et Corpusculaire, Université de Genève, Geneva, Switzerland

g Also at Departament de Fisica de la Universitat Autonoma de Barcelona, Barcelona, Spain

h Also at Departamento de Física Teorica y del Cosmos, Universidad de Granada, Granada (Spain), Spain

i Also at Departamento de Física, Instituto Superior Técnico, Universidade de Lisboa, Lisbon, Portugal

j Also at Department of Applied Physics and Astronomy, University of Sharjah, Sharjah, United Arab Emirates

k Also at Department of Financial and Management Engineering, University of the Aegean, Chios, Greece

l Also at Department of Physics and Astronomy, University of Louisville, Louisville, KY, USA

m Also at Department of Physics and Astronomy, University of Sheffield, Sheffield, UK

n Also at Department of Physics, California State University, Fresno, CA, USA

o Also at Department of Physics, California State University, Sacramento, CA, USA

p Also at Department of Physics, King's College London, London, UK

q Also at Department of Physics, St. Petersburg State Polytechnical University, St. Petersburg, Russia

r Also at Department of Physics, Stanford University, USA

s Also at Department of Physics, University of Fribourg, Fribourg, Switzerland

t Also at Department of Physics, University of Michigan, Ann Arbor, MI, USA

u Also at Dipartimento di Fisica E. Fermi, Università di Pisa, Pisa, Italy

v Also at Giresun University, Faculty of Engineering, Giresun, Turkey

w Also at Graduate School of Science, Osaka University, Osaka, Japan

[x] Also at Hellenic Open University, Patras, Greece

[y] Also at Horia Hulubei National Institute of Physics and Nuclear Engineering, Bucharest, Romania

[z] Also at II Physikalisches Institut, Georg-August-Universität Göttingen, Göttingen, Germany

[aa] Also at Institucio Catalana de Recerca i Estudis Avancats, ICREA, Barcelona, Spain

[ab] Also at Institut für Experimentalphysik, Universität Hamburg, Hamburg, Germany

[ac] Also at Institute for Mathematics, Astrophysics and Particle Physics, Radboud University Nijmegen/Nikhef, Nijmegen, The Netherlands

[ad] Also at Institute for Particle and Nuclear Physics, Wigner Research Centre for Physics, Budapest, Hungary

[ae] Also at Institute of Particle Physics (IPP), Canada

[af] Also at Institute of Physics, Academia Sinica, Taipei, Taiwan

[ag] Also at Institute of Physics, Azerbaijan Academy of Sciences, Baku, Azerbaijan

[ah] Also at Institute of Theoretical Physics, Ilia State University, Tbilisi, Georgia

[ai] Also at Instituto de Física Teórica de la Universidad Autónoma de Madrid, Spain

[aj] Also at Istanbul University, Dept. of Physics, Istanbul, Turkey

[ak] Also at LAL, Université Paris-Sud, CNRS/IN2P3, Université Paris-Saclay, Orsay, France

[al] Also at Louisiana Tech University, Ruston, LA, USA

[am] Also at LPNHE, Sorbonne Université, Paris Diderot Sorbonne Paris Cité, CNRS/IN2P3, Paris, France

[an] Also at Manhattan College, New York, NY, USA

[ao] Also at Moscow Institute of Physics and Technology State University, Dolgoprudny, Russia

[ap] Also at National Research Nuclear University MEPhI, Moscow, Russia

[aq] Also at Physikalisches Institut, Albert-Ludwigs-Universität Freiburg, Freiburg, Germany

[ar] Also at School of Physics, Sun Yat-sen University, Guangzhou, China

[as] Also at The City College of New York, New York, NY, USA

[at] Also at The Collaborative Innovation Center of Quantum Matter (CICQM), Beijing, China

[au] Also at Tomsk State University, Tomsk, and Moscow Institute of Physics and Technology State University, Dolgoprudny, Russia

[av] Also at TRIUMF, Vancouver, BC, Canada

[aw] Also at Universita di Napoli Parthenope, Naples, Italy

[*] Deceased